# KAON PHOTOPRODUCTION IN QUARK MODEL

DISSERTATION

SUBMITTED FOR THE AWARD OF THE DEGREE OF

**Master of Philosophy**

**in**

**Physics**

SUBMITTED BY

Farooq Hussain Bhat

UNDER THE SUPRVISION OF

Dr. A.A. Usmani



DEPARTMENT OF PHYSICS

ALIGARH MUSLIM UNIVERSITY

ALIGARH ( INDIA)

2004

DEPARTMENT OF PHYSICS
ALIGARH MUSLIM UNIVERSITY
ALIGARH – 202 002, INDIA
Tel: (Off.) +91 571 2701001

Dated: May 20, 2004

## CERTIFICATE

The research "Kaon Photoproduction in Quark Model" is carried out by Mr. Farooq Hussain Bhat under my supervision and is suitable for submission for the award of the degree of Master of Philosophy in Physics.

(Dr. Anisul Ain Usmani)
Reader

# Acknowledgement

At the outset I would like to thank Almighty Allah for his invaluable grace over me.

I would like to express my deep gratitude to my supervisor Dr. A. A. Usmani for his inspiring guidance and continuous encouragements throughout the course of this work. I wish to give my special thanks to Prof. S. C. Phatak for the insightful ideas and suggestions, and also for the warm hospitality during my visit at Institute of Physics, Bhubaneswar. I am thankful to our Chairman, Department of Physics, Prof. A. K. Chaubey who has been always supportive and has provided me the facilities to materialize the work for the dissertation. I am immensely thankful to seminar staff for providing me the required journals during my research work. I am very grateful to my family and my friends who always have been helpful and supportive of my pursuit of physics.

The financial assistance from the Council of Scientific and industrial research (CSIR) in the form of Junior Research Fellowship (JRF) is also gratefully acknowledged.

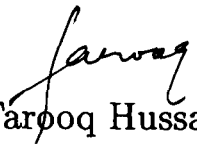

Farooq Hussain Bhat

# Contents

# Chapter 1

# Introduction

The determination of appropriate degree-of-freedom is a fundamental issue central to all branches of physics. A fully microscopic model of a physical structure containing the correct constituents and dynamics may fail frequently to describe the phenomena at a larger scale.Therefore, some global non-fundamental constituent may be useful on this large scale. To understand a physical problem very efficiently it is important to know the relationship between degree-of-freedom and various scales at every level.

In the area of nuclear and subatomic physics, one does come across the above situation; to express the rich and subtle phenomena at subatomic level the fundamental constituents of matter do not manifest themselves as the proper degree-of-freedom.

In 1960s it turned out that hundreds of hadrons known experimentally contained an internal structure and thus they do not represent themselves as fundamental constituents; they rather can be classified according to their constituents at a lower level. These findings marked the developement of a new phase in the description of constituents of matter and strong interaction in terms of quark and gluonic degrees-of-freedom. The concise theory describing the dynamics of quarks and gluons is called as Quantum Chromodynamics (QCD).

At a very High energy limit, that is in the multi GeV region, which can be reached only at a few highly specialized laboratories in the world, the QCD Lagrangian can be solved perturbatively and describes the behaviour of (asymptotically free) quarks and gluons perfectly. But in the lower energy region, coupling constant becomes too large to be solved perturbatively. The increase of coupling constant also implies, that

phenomena at subatomic level can not be described in terms of quarks and gluonic degrees-of-freedom. Hence, only conglomerate or condensate of quarks and gluons can survive in nature like protons, neutrons and mesons.

It is established that QCD is at the basis of composite structure of hadrons, but in many cases QCD lacks appropriate degree-of-freedom to describe hadronic matter at a larger scale e.g. concept of structureless hadrons turns out to be useful in describing properties of nuclei. At Intermediate energies, some of the properties of hadrons are very well explained taking constituent quarks into account leaving out gluons explicitly.

It is an intellectual challenge for human mind, to fully understand the subtilities of subatomic matter and thus to bridge the gap between Nuclear physics, where hadrons are the basic degree-of-freedom, and QCD theory of quarks and gluons.

The main goal of medium-energy physics is to gain deeper insight into the structure of the nucleon or nucleon-nucleon interactions as well as the properties and the behaviour of the first baryonic resonance denoted as N*, where at the subnucleonic level only 'u' and 'd' quarks are involved. Here excitation spectrum of the nucleon reflects its underlying structure from the constituents at a lower level.

Over the last few decades, a substantial amount of information regarding the spectrum of nucleon has been gathered. Most of this information is based on the knowledge gained from electromagnetically induced pion production and pion induced reactions. However it has been realized that pion as a probe may be selective or restrictive with regard to certain type of resonant intermediate states which can be excited. Some recent (constituent) quark model calculations [1, 2, 3, 4], predict far more excited states than observed in pion production experiments. This observation is known as the "missing-resonance" phenomenon in Medium energy physics. So alternate meson production reactions could provide additional information on the excitation spectrum of the nucleon. In particular, involvement of a strange $q\bar{q}$-quark pair in the reaction opens an additional degree-of-freedom, which invokes the investigation of hyperon-nucleon and hyperon-hyperon interactions, the propagation and production of strange hadron resonances and strangeness exchange mechanisms.

The investigation of strangness production from a proton, using real [5, 6] or virtual [5, 6, 7] photons started in the late 1950s, but a comprehensive description of the underlying reaction mechanism is still not available. This uneasy situation, compared to that of pion photoproduction, which is dominated by single nucleonic resonance, might be attributed to the complex role played by the strange quark versus that displayed

by 'u' and 'd' quarks. The introduction of this additional degree-of-freedom leads to the fact that, even close to the threshold, a priori a rather copious number of nucleonic and hyperonic resonances may intervene in the process.

Reactions like $(K^-, \pi^-)$ or $(\pi^+, K^+)$, kaon-nucleon and hyperon-nucleon are the most common methods in the strangeness physics, both experimentally and theoretically [19]. However, because of the strongly interacting nature of both the incident and the outgoing particles with the target nucleons, the extraction of quantitative information remains very model dependent.

An alternative to hadronic processes is the use of electromagnetic probes [7]. Electromagnetic probes are preferred over hadronic probes , due to much better understanding of electromagnetic coupling to nucleon than its hadronic counterpart. Moreover in using electromagnetic probes, distortion in the incident and outgoing channels are largely reduced due to rather weakly interacting nature of both the photon and the $K^+$ with hadrons. This weakness of these interactions justifies their first order description, but results in cross sections are smaller than those of hadronic reactions. In nourishing the hope of evolving towards a subnucleonic description of at least the elementary reactions, efforts to understand the highlights and shortcomings of approaches based on baryonic and mesonic degrees-of-freedom are of special interest.

Our knowledge of the kaon-baryon interaction is much poorer than our knowledge of the pion-nucleon force, intensified by the uncertainity in the kaon-hyperon-nucleon coupling constants.The effort in understanding kaon photoproduction off the nucleon is expected to provide a convenient means in our knowlegde of the fundamental kaon-hyperon-nucleon(KYN) coupling constants, as well as reaction mechanism, electromagnetic form factors of the kaon or hyperon, or even form factors at the hadronic vertices. Besides, it serves as a first step in further studies of strangeness in hadronic aggregates. Using nucleus as the target one can study the hypernuclear spectroscopy and hyperon-nucleon (YN) interaction.

Efforts to model kaon photoproduction processes started back in the 1960s by Kuo [8] and Thom [9] which was the start of a long series of theoretical efforts in this field [10-20]. The earliest works were lacking the reliable data base. In those days, pioneering kaon photoproduction experiments were carried out at Bonn, Tokyo, Cornell and Caltech [19-24] but experimental facilities covered only a limited range of energy above the kaon production threshold. Matters got worsen further due to low counting rates, yielding cross sections of the order of microbarns, compared to $\pi$- production,

characterized by cross sections in the millibarn range. After nearly three decades of investigation, the field of electromagnetic production of strangeness have been dormant since the mid 1970s mainly due to lack of adequate experimental facilities and a seemingly complicated elementary reaction mechanism. But with the onset of new generation of electron accelerators and associated detectors,which provide continous, high-current and polarized beams in the energy range of few GeVs, there has been considerable recent interest in studying meson photo- and electroproduction off nucleons. At present high duty electron and photon facilities like CEBAF, ELSA, MAMI, Spring-8, GRAAL, ESRF, Bates and LEGS provide data for electro- and photoproduction of mesons with unprecedented accuracy. With the onset of SAPHIR collaboration at Bonn [25, 26] first extensive and accurate data base got released for all three $\gamma p \to K^+\Lambda$, $K^+\Sigma^0$, $K^0\Sigma^+$, reactions. These experimental facilities provide us a wonderful opportunity to study the structure of baryon resonances and a challenge to extract reliable information from the data available to understand the reaction mechanism in terms of QCD and in an as model independent way as possible.

The photoproduction reactions that are being, or will be studied in the near future at above mentioned laboratories, will focus on the following reactions:

$$\gamma + p \to K^+ + \Lambda, \tag{1.1}$$

$$\gamma + p \to K^+ + \Sigma^0, \tag{1.2}$$

$$\gamma + p \to K^0 + \Sigma^+. \tag{1.3}$$

Reaction (1.1) is by far the one most studied, both theoretically [5-7] and experimentally [9,19,20,21,23,24] including polarization observable measurements [22, 27]. Also this is rather simple one, since there are only four indpendent Lorentz- and guage-invariant terms for real photons. There are less extensive investigations of the reaction (1.2), and process (1.3) has up to now received very little consideration, probably because of experimental difficulties in identifying the final state particles.

In general, the theoretical description of meson photoproduction goes along two major paths. On one hand, there are parton based models. Thereby, a (constituent) quark model is at the basis of calculations of the reaction dynamics [32-34]. The partonic constituents can also be taken into account along the lines proposed by Regge theory [18] which is a high energy theory or in chiral models which are a low energy approximation of the QCD formalism [28, 29]. The other method of tackling the

problem is by starting from purely hadronic degrees-of-freedom, where hadrons are treated as effective particles with specific properties [15, 30] . From this approach one is hopeful to reach a deeper level of understanding of the "phase transformation" between low and high energy descriptions of subatomic matter.

The description of the reaction $p(\gamma, K^+)\Lambda^0$, $\Sigma^0$ in terms of hadronic degrees-of-freedom and their excited state is referred to as the "Isobaric Model". By far this is the most extensively used approach between threshold and roughly $E_\gamma^{lab} = 2$ GeV. Following the pioneering works by Thom [9] and Renard and Renard [12], revived in early 1980s by Hsiao and Cotanch [31] and Adelseck, Bennhold and Wright [11]. All these formalisms use the Feynman diagrammatic techniques. After 1990, three major models based on isobaric approaches, have been published. The first one by Adelseck-Saghai [5] focuses on the reaction $\gamma + p \rightarrow K^+ + \Lambda^0$ for $E_\gamma^{lab} \leq 1.5$ GeV. The second one, by Williams, Ji and Cotanch [6], investigates the above reactions (1.1) and (1.2) including electroproduction of $K^+$ i.e.

$$e + p \rightarrow e' + K^+ + \Lambda^0, \tag{1.4}$$

$$e + p \rightarrow e' + K^+ + \Sigma^0, \tag{1.5}$$

and radiative capture processes i.e.

$$K^- + p \rightarrow \gamma + \Lambda^0, \tag{1.6}$$

$$K^- + p \rightarrow \gamma + \Sigma^0. \tag{1.7}$$

The model extends the energy range to $E_\gamma^{lab} \leq 2.1$ GeV. The final and recent one, by Mart, Bennhold and Hyde-Wright [14] studies K$\Sigma$ photoproduction channels emphasizing on the charged $\Sigma$ production in the same energy range as Williams [6].

But despite its long history and the large amount of both experimental and theoretical efforts, a complete understanding of the $p(\gamma, K^+)\Lambda^0$, $\Sigma^0$ reaction mechanism is elusive in this model. One of the major reasons for this obscurity is that the reaction is fully located in the so called third resonance region. There are more than twenty resonances likely to participate in the reaction, from the kinematical point of view. A number of these resonances are poorly characterized. Thus it is believed that all those have large widths of few MeV, resulting in a broad energy smearing of every state . This creates a problem in theoretical description since various resonances overlap in the same region, giving an erratic interference pattern. Unlike this, in the processes

p($\gamma$,$\pi$)N or p($\gamma$,$\eta$)p near threshold, one does not face similar difficulties since their dynamics is dominated by single (isolated) resonance.

Another major problem for the models aiming to describe p($\gamma$,$K^+$)Y process, is the description of non-resonant or background diagrams along with the limited knowledge regarding various resonance contributions. So, some model dependence in order to determine background contributions is necessary.

This dissertation work consists of four chapters including introduction. In the second chapter the kinematics of the reaction $\gamma + P \rightarrow \Lambda + K^+$, the theoretical models and techniques used to study latter are discussed. The form factor calculation and amplitude calculation is done in chapter third. Finally the results are discussed in fourth chapter.

# Chapter 2

# Kinematics and Various Theoretical Models

This chapter reviews the essential ingradients for describing kaon photoproduction. First, we introduce the general formalism for describing the photoproduction of kaon and then we discuss various models used to study the kaon photoproduction.

## 2.1 General Formalism

The formlism for the photoproduction of pseudoscalar mesons has been given in many publications [5, 35, 36]. In the following we describe some essential formulae for kinematics and several commonly used amplitudes.

### 2.1.1 Kinematics

The reaction for kaon photoproduction on a proton is:

$$\gamma(k) + p(p_i) \rightarrow K^+(q) + \Lambda(p_f) \tag{2.1}$$

where for each particle four-momentum is given in parenthesis and they satisfy $p_i^2 = m_p^2, p_f^2 = m_\Lambda^2, q^2 = m_{K^+}^2$ where $m_p$, $m_\Lambda$ and $m_{K^+}$ indicate the masses of proton, $\Lambda$ and kaon respectively. For photoproduction photon is real ($k^2$=0, k is the four-momentum of photon). The invariant Mandelstam variables are given as

$$s = (k + p_i)^2 = (q + p_f)^2,$$
$$u = (k - p_f)^2 = (q - p_i)^2,$$

$$t = (q-k)^2 = (p_i - p_f)^2, \tag{2.2}$$

which is subject to the constraint $s+u+t = m_p^2 + m_\Lambda^2 + m_{K^+}^2 + k^2$. It is easier to work in the $\gamma p/\Lambda K^+$ center-of-mass (CM), where energy and momentum of each particle can be written as

$$k = (k_0, \mathbf{k}), p_i = (E_i, \mathbf{p_i}) = (E_i, -\mathbf{k}), q = (\omega, \mathbf{q}),$$

$$p_f = (E_f, \mathbf{p_f}) = (E_f, -\mathbf{q}). \tag{2.3}$$

The relations(2.2), in the CM system become

$$s = W^2 = (E_i + k_0)^2, \tag{2.4}$$

$$u = k^2 + m_\Lambda^2 - 2k_0E_f - 2|\,\mathbf{q}\,||\,\mathbf{k}\,|x, \tag{2.5}$$

$$t = m_{K^+}^2 + k^2 - 2k_0\omega + 2|\,\mathbf{q}\,||\,\mathbf{k}\,|x, \tag{2.6}$$

where

$$x = \cos\theta = \frac{\mathbf{q}\cdot\mathbf{k}}{|\,\mathbf{q}\,||\,\mathbf{k}\,|}. \tag{2.7}$$

Here, $m_\Lambda$ and $m_{K^+}$ are the masses of $\Lambda$, $K^+$ and $E_f$ and $\omega$ are their energies respectively, $\theta$ is the CM scattering angle and W is the total CM energy. In the CM momenta and energies of initial and final states can be expressed in terms of $W = \sqrt{s}$ and $k^2$ as

$$k_0 = \frac{W^2 - m_p^2 + k^2}{2W},\ E_i = \frac{W^2 - k^2 + M^2}{2W}, \tag{2.8}$$

$$\omega = \frac{W^2 + m_{K^+}^2 - m_\Lambda^2}{2W},\ E_f = \frac{W^2 - m_{K^+}^2 + m_\Lambda^2}{2W}, \tag{2.9}$$

$$|\,\mathbf{p_i}\,| = |\,\mathbf{k}\,| = \frac{1}{2W}\sqrt{[(W+m_p)^2 - k^2][(W-m_p)^2 - k^2]} \tag{2.10}$$

$$|\,\mathbf{p_f}\,| = |\,\mathbf{q}\,| = \frac{1}{2W}\sqrt{[(W+m_\Lambda)^2 - m_{K^+}^2][(W-m_\Lambda)^2 - m_{K^+}^2]} \tag{2.11}$$

where the quantities involved are already defined.

For photoproduction, $k^2 = 0$, and the relation between the energy $E_\gamma$ of the photon in the lab. frame and CM energy is

$$E_\gamma = \frac{W^2 - m_\Lambda^2}{2m_\Lambda}. \tag{2.12}$$

At the threshold of kaon photoproduction, the energy in the CM is just enough to produce final hyperon and kaon at rest, i.e., $W_{th}$=m$_\Lambda$ +m$_{K^+}$. Therefore, the threshold energy in the lab. frame for the incident photon is given by

$$E_\gamma^{(th)} = \frac{W_{(th)}^2 - m_\Lambda^2}{2m_\Lambda}. \tag{2.13}$$

The proof of the above relations is given in the Appendix A.

### 2.1.2 Photoproduction amplitudes

In this section, we present the most commonly used amplitudes in the description of kaon photoproduction. In all cases there are four independent complex amplitudes, differing in their good quantum number basis. Each type of amplitude shows its convenience in different aspects of calculations.

#### Invariant amplitudes

The S-matrix[36]for the kaon photoproduction process(2.1)can be writen as

$$S_{fi} = \frac{1}{2\pi}\sqrt{\frac{Mm}{4\omega k_0 E_i E_f}} i\mathcal{M}_{fi}\delta^4(p_f + q - p_i - k), \tag{2.14}$$

from which the cross section follows as

$$d\sigma = (2\pi)^4 \frac{Mm}{4E_f\omega\sqrt{[(p_i\cdot k)^2 - p_i^2k^2]}} \frac{d^3p'}{(2\pi)^3}\frac{d^3q}{(2\pi)^3} \mid \mathcal{M}_{fi} \mid^2 \delta^4(p_f + k - p_i - q). \tag{2.15}$$

The Lorentz-invariant matrix element $iM_{fi}$ can be decomposed as

$$i\mathcal{M}_{fi} = \overline{u}_f(\mathbf{p_f})\epsilon_\mu \mathbf{O}^\mu u_i(\mathbf{p_i}), \tag{2.16}$$

where $u_i$ and $\overline{u}_f$ are respectively the Dirac spinors for the initial and final baryons, $\mathbf{O}^\mu$ describes the current operator produced by the strongly intracting hadrons, and $\epsilon_\mu$ is the photon polarization four vector. The invariant matrix element is often expanded [37] as

$$i\mathcal{M}_{fi} = \overline{u}_f(\mathbf{p_f})[\sum_{j=1}^{6} A_j(s,t,u,k^2)\mathcal{M}_j]u_i(\mathbf{p_i}), \tag{2.17}$$

where the $A_{j's}$ are Lorentz invariant scalar functions of the Mandelstam variables and $k^2$, and the $\mathcal{M}_{j's}$ are the six guage invariant matrices [9] given by

$$\begin{aligned}
\mathcal{M}_1 &= \frac{1}{2}\gamma_5(\gamma\cdot\mathbf{k}\gamma\cdot\epsilon - \gamma\cdot\epsilon\gamma\cdot\mathbf{k}) \\
\mathcal{M}_2 &= 2\gamma_5(\epsilon\cdot\mathbf{p_i}\mathbf{k}\cdot\mathbf{p_f} - \mathbf{k}\cdot\mathbf{p_i}\epsilon\cdot\mathbf{p_f}) \\
\mathcal{M}_3 &= \gamma_5(\gamma\cdot\epsilon\mathbf{k}\cdot\mathbf{p_i} - \gamma\cdot\mathbf{k}\epsilon\cdot\mathbf{p_i}) \\
\mathcal{M}_4 &= \gamma_5(\gamma\cdot\epsilon\mathbf{k}\cdot\mathbf{p_f} - \gamma\cdot\mathbf{k}\epsilon\cdot\mathbf{p_f}) \\
\mathcal{M}_5 &= 2\gamma_5(\epsilon\cdot\mathbf{k}\mathbf{k}\cdot\mathbf{q} - \mathbf{k}^2\epsilon\cdot\mathbf{q}) \\
\mathcal{M}_6 &= \gamma_5(\epsilon\cdot\mathbf{k}\gamma\cdot\mathbf{k} - \mathbf{k}^2\gamma\cdot\epsilon).
\end{aligned} \tag{2.18}$$

Here $\mathcal{M}_5$ and $\mathcal{M}_6$, which contain the additional spin degrees of freedom for the virtual photon, are needed for electroproduction only. Thus for photoproduction only first four complex amplitudes are needed

### Chew-Goldberger-Low-Nambu(CGLN) amplitudes

The matrix elements appearing in equation(2.17) can be written in a two component form by expressing the $\gamma$ matrices in terms of the Pauli $\sigma$-matrices, and the Dirac spinors in terms of the two component spinors:

$$\mathcal{M}_{fi} = \frac{4\pi W}{\sqrt{Mm}}\chi_f^\dagger\mathcal{F}\chi_i \tag{2.19}$$

where the $\chi_i$, $\chi_f$ are the Pauli spinors for the initial and final baryon, and the factor $\frac{4\pi W}{M}$ has been introduced in the definition of $\mathcal{F}$ which is an operator in spin space. For photoproduction, $\mathcal{F}$ is often written in the CGLN form [38] which involves the four complex opertors $\mathcal{F}_1,\cdots\mathcal{F}_4$:

$$\mathcal{F} = i\boldsymbol{\sigma}\cdot\boldsymbol{\epsilon}\mathcal{F}_1 + \boldsymbol{\sigma}\cdot\hat{\mathbf{q}}\,\boldsymbol{\sigma}\cdot(\hat{\mathbf{k}}\times\boldsymbol{\epsilon})\mathcal{F}_2 + i\boldsymbol{\sigma}\cdot\hat{\mathbf{k}}\,\hat{\mathbf{q}}\cdot\boldsymbol{\epsilon}\mathcal{F}_3 + i\boldsymbol{\sigma}\cdot\hat{\mathbf{q}}\,\hat{\mathbf{q}}\cdot\boldsymbol{\epsilon}\mathcal{F}_4 \tag{2.20}$$

for electroproduciton,all six amplitudes appear

$$\begin{aligned}
\mathcal{F} = {} & i\boldsymbol{\sigma}\cdot\mathbf{b}\mathcal{F}_1 + \boldsymbol{\sigma}\cdot\hat{\mathbf{q}}\,\boldsymbol{\sigma}\cdot(\hat{\mathbf{k}}\times\mathbf{b})\mathcal{F}_2 + \mathbf{i}\boldsymbol{\sigma}\cdot\hat{\mathbf{k}}\,\hat{\mathbf{q}}\cdot\mathbf{b}\mathcal{F}_3 \\
& + i\boldsymbol{\sigma}\cdot\hat{\mathbf{q}}\,\hat{\mathbf{q}}\cdot\mathbf{b}\mathcal{F}_4 - \mathbf{i}\boldsymbol{\sigma}\cdot\hat{\mathbf{q}}\,\mathbf{b}_0\mathcal{F}_5 - \mathbf{i}\boldsymbol{\sigma}\cdot\hat{\mathbf{k}}\,\mathbf{b}_0\mathcal{F}_6.
\end{aligned} \tag{2.21}$$

Here

$$b_\mu \equiv \epsilon_\mu - \frac{\boldsymbol{\epsilon}\cdot\hat{\mathbf{k}}}{|\,\mathbf{k}\,|}k_\mu$$

.

## 2.2 Theoretical Models

It is believed that quantum chromodynamics (QCD) is the basic theory of strong interaction, it was born by combining the Yang and Mills non-Abelian guage theory with the quark model. It has got
$SU_L(N_f) \otimes SU_R(N_f)$ symmetry ($N_f$, flavour number) in a massless limit of quark and is non-perturbative in the intermediate energy region. In the non-perturbative vacuum, the $SU_L(N_f) \otimes SU_R(N_f)$ symmetry is spontaneously broken down to $SU_V(N_f)$ and massless Goldstone bosons, which are pseudoscalar mesons with spin and parity $J^p = 0^-$, appear. Due to nonperturbative property of QCD in intermediate energy region, nuclear force remains elusive by directly tackling QCD. Therefore, an effective theory which has the basic symmetry of QCD is used to investigate the nuclear force, since pseudoscalar meson plays an important role in intermediate energy nuclear physics, using such an effective theory in understanding its property is an inevitable study in the nuclear physics at this energy region. The photo- or electro-production of pseudoscalar mesons is a reliable source of information on the property of pseudoscalar meson interaction with nuclei due to weak absorption of real or virtual photon as probing particle than the hadron induced reactions. On the other hand kaon electroproduction on nuclei is studied with more interest for the hypernuclei production. Most of the studies on kaon photoproduction have been performed using isobaric Models [43, 9, 12, 11, 14, 40, 41, 5, 10, 13, 6, 24, 39, 42, 15, 16, 44], dispersion relations[45, 46], multipole analysis [47] and quark based models [48, 49, 50]. In the dispersion relation theory or multipole analysis, amplitudes are obtained in the $K - \Lambda$ centre of mass (CM) reference frame, so that transforming them into other frames is cumbersome and ambigious. In addition, it is difficult to discuss non-local and off-shell effects, which turned out to play a significant role in nuclear applications of the elementary kaon photoproduction amplitudes. Moreover, due to higher energy threshold of the reaction, in dispersion theory , the multipion channels $\gamma + N \rightarrow N + m\pi$ with m=1 to 4 are already open for $K^+\Lambda$ process. The inclusion of these reactions leads to very complicated integral equations among the partial amplitudes. And to solve these equations unjustifiable approximations are needed. Advantage of using quark-based model is to describe the reaction by an unified scheme and to explain the reaction well with relatively less parameters than other models. But nuclear application is also not easy. Finally isobaric models are widely used methods to investigate the kaon photoproduction between

threshold and roughly $E_\gamma^{lab} = 2.0$ Gev region.

### 2.2.1 Isobaric Model and effective Lagrangian Formalism

The term "Isobar" was originally used to describe nucleon excited state which have masses close to nucleons but have different quantum numbers (e.g. the spin $J = \frac{1}{2}$ and isospin $I = \frac{3}{2}$ for the $\Delta$ (1232), opposed to $J = \frac{1}{2}$ and $I = \frac{1}{2}$ for nucleons). Nowadays in the isobaric model, the isobar stands for general baryon resonances or excited states.

In an isobar model, the physical degrees- of-freedom are the hadrons and their excited states. In such a frame work, the meson photopoduction reactions are modelled with the aid of effective Lagrangian formalism, which is at the basis of isobar model.The non-resonant contributions, which correspond to the Born terms for proton, kaon and hyperon exchange (shown in Fig.2.1) are calculated by lowest-order perturbation theory. Using Feynman diagrammatic techniques, the resonant amplitudes are derived by evaluating vertex functions from an effective Lagrangian and applying corresponding exchange particle operators. The resonant terms for the exchange of the $N^*$, $\Delta^*$, $Y^*$, and $K^*$ resonances (shown in Fig.2.1) are evaluated by the same procedure as nonresonant terms with the propagators of resonances described by a Breit-Wigner form. Every (intermediate) particle in the reaction dynamics is treated as an effective field with its own characteristics like mass, photocoupling amplitudes and strong decay widths. That means in effective Lagrangian approach effect of the internal structure of hadron is not considered.

In this approach, the Born terms and the contributions from the excitation of intermediate resonant states, above as well as below threshold, are represented by the lowest order Feynman diagrams. To calculate the reaction amplitude for a given process, the dominant Feynman diagram have to be identified . Initially only the first order terms known as the "tree level" diagrams are taken into account (Fig.2.1) and additional loops are not introduced.

But there is one important drawback, with these first order terms that is, the final state interaction effects , generated through the rescattering of the final state particles, are not taken into account . Rescattering contributions such as $\gamma p \rightarrow \pi N^* \rightarrow KY$ are of second order and for example can be handled in a full coupled-channel analysis [51]. Recent estimates of the effect of the coupled channel-mechanisms on the $p(\gamma, K^+)\Lambda$ cross section has been worked out to be 20% [52], which is a substantial effect. However

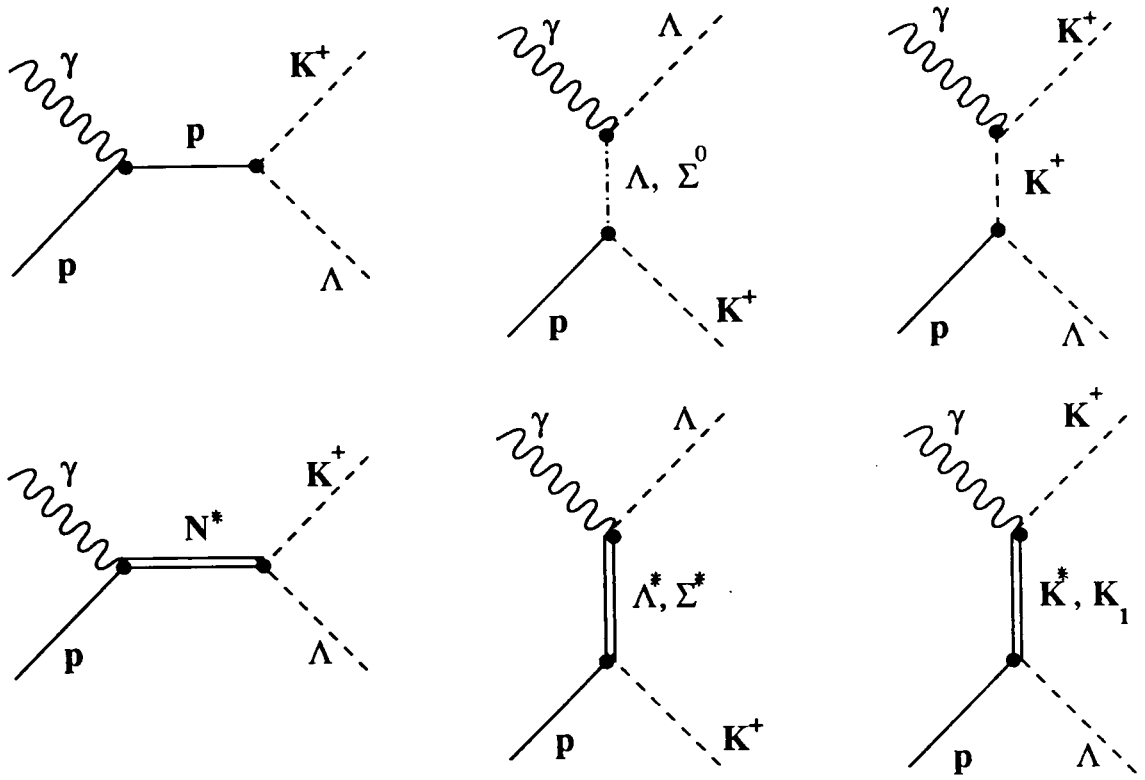


Figure 2.1: Diagrams contributing to the $p(\gamma, K^+)\Lambda$ process at tree level. The upper row corresponds to the Born terms in which a proton is exchanged in the s-channel, a $\Lambda$ or $\Sigma^0$ in the u-channel and a K in the t-channel.The lower row shows the resonant terms for the exchange of the $N^*$, $K^*$ and $Y^*$ resonances.

due to uncertainties inherent to coupled-channel approaches, such as unknown phase-shifts and off-shell rescattering ambiguities, the tree level diagrams constitute the major part of the $p(\gamma, K^+)\Lambda$ reaction dynamics.

The resonant terms refer exclusively to the S-channel (nucleon) resonance contributions. These are $S_{11}(1650)$, $P_{11}(1710)$, $P_{13}(1710)$,and $D_{13}(1895)$ resonances unless specified otherwise. The Born terms, two t-channel contributions involving the vector meson $K^*(892)$ and the axial vector mesons $K_1(1270)$ and the u-channel hyperon resonances, all contribute to what is called background. Note that the parameters for resonances exchange in photoproduction are the products of photon-couplings and hadronic couplings (called photo-hadronic couplings in brief). Unlike pion-photoproduciton where the hadronic couplings are predetermined by $\pi$N scattering experiments we can not do the same for kaon photoproduction since a KY$\rightarrow$KY reaction is not feasible experimentally. Therefore photon and hadronic couplings in kaon photoproduction are

not separable and we can only determine their products, photo-hadronic couplings.

As is well known there are two coupling types of kaon and baryon with $J = \frac{1}{2}$ in strong vertex. One is pseudoscalar(PS) coupling where a kaon-nucleon-hyperon (KNY) vertex is described by $g_{KNY}\gamma_5$ with a PS coupling constant of KNY, $g_{KNY}$ and the other is a pseudovector(PV) coupling in which the KNY vertex is described by $\frac{f_{KNY}}{M_N+M_\gamma}/q\gamma_5$, where $f_{KNY}$, $M_N$, $M_\gamma$ and q are a PV-coupling constant, a nucleon mass, a hyperon mass, and an outgoing kaon-four momentum, respectively. This issue i.e. use of PS or PV coupling has been studied by several authors [39, 53, 54] , but neither of the two possible schemes has as yet been identified as favourable. Moreover the contribution of the spin$\frac{1}{2}$ particles are comparable to those of particles with other spins. Therefore, the difference between the PV and PS coupling schemes in this reaction is expected to be much larger than in the pion-photoroduction.

Neverthless, until now , most of the calculations based on an isobaric model were carried out by the PS coupling scheme. Some works [16, 39, 55] were done by using the PV coupling, but they used models oversimplified.

The interaction Lagrangians depend on an effective coupling that determine the strengths of the corresponding underlying interaction. In an effective field theory, the coupling constants for each of the individual resonances are not determined by the theory itself, rather they are treated as free parameters and must be extracted by performing a global fit of the model calculations to variable data base.

### 2.2.2 Dispersion Theory and Dispersion Relations

The methods of computing transition amplitudes using a weak-coupling perturbation expansion in terms of the electric charge $\alpha = \frac{1}{137}$, for instance, are of little help when we turn to the realm of strong interactions. The "dispersion relations" makes one of the most successful approaches to the strong-interaction problem which draws on the exploration of the complex plane. The local structure of the field theory commutation relations and the field equations pose certain restrictions on the behaviour of scattering amplitudes, studied as function of energy and momentum transfer, when these variables are analytically continued from the physical domain of values achieved in the laboratory to an unphysical domain in the complex plane. From these restrictions useful relations for evaluating these amplitudes or expressing them in terms of other measurable quantities are then constructed [56].

The real significance of the dispersion relations lies in the fact that they are a direct consequence of assuming that the particular system obeys causality, which is awkward to define precisely but the general meaning is that the effect can not precede the cause.

### Causality and Kramers-Kronig Relations

It was Kronig [57] who first drew attention to the fact that the requirement, that signals not propagate at supervedic speed, might impose limitations on the S-matrix. This prohibition is generally referred to as the principle of microcausality. This technique got inspired from Kramers-Kronig relation in optics, which expresses the real part of the amplitude for forward scattering by atoms of the light of a fixed frequency $\omega$ as an integral over the cross section for the absorption by atoms of all frequencies. In macroscopic terms, the real part of the index of the refraction of a medium of such atoms is given by an integral over all frequencies of the imaginary part. This relation is described by establishing that the forward-scattering amplitude is analytic in the upper half of the complex $\omega$ plane, a mathematical property based up on the physical limitation that electromagnetic signals can not travel with a speed greater than that of light.

Let us consider a monochromatic light wave

$$a_{inc}(\omega)e^{-i\omega(t-x)},$$

propagating up the x-axis and impinging up on a scattering centre. Then relation between scattered and incident wave is

$$a_{scatt}(\omega) = f(\omega)a_{inc}(\omega),$$

where $f(\omega)$ is forward scattering amplitude and scattered wave becomes asymptotically

$$a_{scatt}(x,t) \rightarrow_{x\rightarrow\infty} a_{scatt}(\omega)\frac{e^{-i\omega(t-x)}}{x}.$$

Considering waves of different frequencies to form a general packet, we write for the incident and forward scattered waves

$$A_{inc}(x,t) = \int_{-\infty}^{\infty} d\omega' a_{inc}(\omega')e^{-i\omega'(t-x)} \tag{2.22}$$

$$A_{scatt}(x,t)\rightarrow_{x\rightarrow\infty}\frac{1}{x}\int_{-\infty}^{\infty} d\omega' f(\omega')e^{-i\omega'(t-x)} \tag{2.23}$$

Let us suppose that Eq.(2.22) represents a signal which vanishes for $x > t$. This physical condition implies a mathematical one on the Fourier amplitudes

$$a_{inc}(\omega) = \frac{1}{2\pi}\int_{-\infty}^{0} dx A_{inc}(x,0)e^{-i\omega x} \tag{2.24}$$

where the upper limit comes from the condition that $A_{inc}(x,0)$ vanishes for $x > 0$. We observe that $a_{inc}(\omega)$ may be analytically continued into the upper half of the complex $\omega$ plane, since for $\omega \to \omega + i \mid \gamma \mid$

$$a_{inc}(\omega + i \mid \gamma \mid) = \frac{1}{2\pi}\int_{-\infty}^{0} dx A_{inc}(x,0)e^{-i\omega x - |\gamma||x|} \tag{2.25}$$

and the integral is absolutely convergent. The physical demand of causality is

$$A_{scatt}(x,t) = 0\ ,\ x > t$$

that is no signal propagates to $x > t$, ahead of the incident wave front. Using same argument as above, we conclude from equation(2.23) that $a_{inc}(\omega)f(\omega)$ may also be analytically continued in the upper half plane. Consequently, $f(\omega)$ is analytic in the upper half plane and we may write a Cauchy relation

$$f(z) = \frac{1}{2\pi i}\int_c d\omega' \frac{f(\omega')}{\omega' - z} \tag{2.26}$$

for any $z = \omega + i \mid \gamma \mid$ in the upper half plane and for C the contour drawn in Fig.2.2.Letting z approach real values $\omega$ from the upper half plane we find

$$f(\omega) = \lim_{\epsilon \to 0^+} f(\omega + i\epsilon) = \frac{1}{2\pi i} P\int_{-\infty}^{\infty} d\omega' \frac{f(\omega')}{\omega' - \omega} + \frac{1}{2}f(\omega) + \frac{1}{2}C_\infty \tag{2.27}$$

where $P\int$ indicates the principal value of the integral along the real axis from -$\infty$ to $\infty$ in the Fig.2.2. The half-circuit around the pole at $\omega' = \omega$ gives the second term, and the contribution from the infinite semicircle is the complex quantity $C_\infty$=$C_\infty$+i$C'_\infty$. The real and imaginary parts of Eq.(2.27) are

$$Ref(\omega) = \frac{1}{\pi} P\int_{-\infty}^{\infty} d\omega' \frac{Imf(\omega')}{\omega' - \omega} + C_\infty \tag{2.28}$$

$$Imf(\omega) = -\frac{1}{\pi} P\int_{-\infty}^{\infty} d\omega' \frac{Ref(\omega')}{\omega' - \omega} + C'_\infty \tag{2.29}$$

Eq.(2.28) is the real part of the following equation

$$f(\omega) = \lim_{\epsilon \to 0^+} f(\omega + i\epsilon) = \lim_{\epsilon \to 0^+} \frac{1}{Pi}\int_{-\infty}^{\infty} d\omega' \frac{Imf(\omega')}{\omega' - \omega - i\epsilon} + C_\infty. \tag{2.30}$$

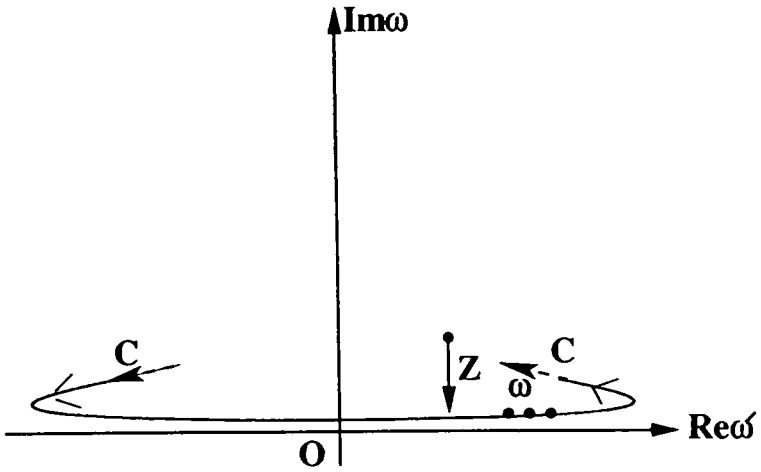


Figure 2.2: Contour in the upper half $\omega'$ plane for cauchy relation 2.26

In writing above equation we used $(x-i\epsilon)^{-1}=\mathrm{P}\frac{1}{x}+\mathrm{i}\Pi\delta(x)$ in the limit $\epsilon \to 0^+$, Eq.(2.30) is the more general form of a dispersion relation.

The contribution $C_\infty$ from the big semicircle at $\infty$ will not vanish if $f(\omega)$ does not approach zero as $\omega \to \infty$. It may be suppressed by making "subtractions". We may consider the amplitude $f(\omega)/\omega$ instead of $f(\omega)$ in constructing the Cauchy relation (Eq.2.26): the only difference is that $f(\omega)$ has an extra pole at $\omega = 0$ and better behaviour at $\infty$. If $f(\omega)$ is bounded by a constant as $\omega \to \infty$, we have then instead of Eq.(2.28)

$$Re\frac{f(\omega)}{\omega} = Re\frac{f(0)}{\omega} + \frac{1}{\pi}P\int_{-\infty}^{\infty} d\omega' \frac{Imf(\omega')}{\omega'(\omega'-\omega)} \tag{2.31}$$

which is called dispersion relation with one subtraction. With the stronger convergence assumption that $f(\omega) \to 0$ as $\omega \to \infty$, we have the no subtraction version of Eq.(2.28) with $C_\infty$=0.

In either of the form (Eq.2.28 or Eq. 2.31), the dispersion relation permits computation of the complete scattering amplitude from a knowledge of the imaginary part, plus its value at $\omega$=0 if a subtraction is necessary [and derivatives of $f(\omega)$ at $\omega$=0, if more subtractions are required]. But as compensation for this advantage one needs to know imaginary part for all frequencies in order to calculate the complete scattering amplitude at any one frequency.

In the present case this hardly is a disadvantage because the imaginary part of the forward-scattering amplitude for positive frequencies $\omega$ is related by the optical

theorem to the total cross section for absorption of light of that frequency. We obtain

$$Imf(\omega) = \frac{\omega}{4\pi}\sigma_{tot}(\omega) \tag{2.32}$$

with $\omega > 0$. Furthermore , we can remove the range of negative $\omega$ from the dispersion integral (Eq.2.28,2.29) by observing from Eq.(2.22) and Eq.(2.23) that reality of the incident and scattered waves requires

$$a_{inc}(-\omega) = a^*_{inc}(\omega) \tag{2.33}$$

$$f(-\omega) = f^*(\omega). \tag{2.34}$$

Therefore,

$$Imf(-\omega) = -Imf(\omega). \tag{2.35}$$

The real part of $f(\omega)$ is even and the imaginary part is odd. However the dispersion integral need to be taken over the positive-frequency spectrum only:

$$Ref(\omega) = \frac{2}{\pi}P\int_0^\infty \frac{\omega' d\omega'}{(\omega'^2 - \omega^2)} Imf(\omega') \tag{2.36}$$

or

$$Ref(\omega) = Ref(0) + \frac{2\omega^2}{\pi}P\int_0^\infty \frac{d\omega' Imf(\omega')}{\omega'(\omega'^2 - \omega^2)} \tag{2.37}$$

Thus with the use of optical theorem Eq.(2.32) we arrive at a definite prediction based generally upon causality in the propagation of light signals and upon conservation of probability (unitarity) in the scattering process via the optical theorem. The real part of the coherent forward scattering of light in a medium of atoms, that is, the real part of the index of refraction, can be computed by the dispersion relation by either calculating or measuring the simpler quantity describing the absorption of light in the medium. This relation

$$Ref(\omega) = Ref(0) + \frac{\omega^2}{2\pi^2}P\int_0^\infty \frac{d\omega' \sigma_{tot}(\omega')}{(\omega'^2 - \omega^2)} \tag{2.38}$$

is the original Kramers-Kronig relation.

### 2.2.3 Multipole Analysis

For convenient analysis of the experimental data and to study individual baryon resonances, photoproduction amplitudes are often expressed in terms of two types of

Table 2.1: Multipole states for pseudoscalar meson photoproduction

| Final state $l$ | Total j | Initial state L | Parity $\mathcal{P} = -(-1)^l$ | Amplitudes $\phi_j = l \pm \frac{1}{2}$ | $l_{min}$ |
|---|---|---|---|---|---|
| $l$ | $l + \frac{1}{2}$ | j + $\frac{1}{2} = l + 1$ | $(-1)^L$ | $E_{l_+}$ | 0 |
| $l$ | $l$ - $\frac{1}{2}$ | j - $\frac{1}{2} = l$ - 1 | $(-1)^L$ | $E_{l_-}$ | 2 |
| $l$ | $l + \frac{1}{2}$ | j - $\frac{1}{2} = l$ | $-(-1)^L$ | $M_{l_+}$ | 1 |
| $l$ | $l$ - $\frac{1}{2}$ | j + $\frac{1}{2} = l$ | $-(-1)^L$ | $M_{l_-}$ | 1 |

multipoles, electric ($E_{l\pm}$) and magnetic ($M_{l\pm}$). Each electric or magnetic multipole amplitude ($E_{l\pm}$), ($M_{l\pm}$), which refers to an electric or magnetic transition to a meson-baryon final state with orbital angular momentum l and definit parity. For electroproduction, there are additional longitudinal($L_{l\pm}$) (or alternatively, scalar ($S_{l\pm}$) types of multipoles. The multipole amplitudes are classified according to the total angular momentum $J = l + \frac{1}{2}$ and the photon state, which can be either electric (with parity $(-1)^L$) or magnetic (with parity $(-1)^{(L+1)}$), where L is the total angular momentum of the photon. In Table 2.1 , these multipole transitions [51] for photoproduction and their associated quantum numbers are shown. It is the use of good total angular momentum and definite parity quantum numbers that make these multipole amplitudes particularly useful for analysis of baryon resonances, for which the J and parity are the good quantum numbers.

In the multipole analysis [47] the total angular momentum $J = l \pm \frac{1}{2}$ is composed of a resonating and a smooth background contribution :

$$E_{l\pm} = A^{res}_{l\pm} + A^{b}_{l\pm} \tag{2.39}$$

and analogously for $M_{l\pm}$. For resonating amplitude a generalized Breit-Wigner form [64] is

$$A^{res}_{l\pm} = \frac{1}{\sqrt{qk}} \frac{1}{\sqrt{j_\gamma(j_\gamma+1)}} \frac{\Gamma_{if}}{\Gamma} \{ \frac{W_R \Gamma}{W_R^2 - W^2 - iW_R\Gamma} e^{2i\delta_\infty} + sin\delta_\infty e^{i\delta_\infty} \}, \tag{2.40}$$

where $j_\gamma = l_\pm + 1$ for $E_{l\pm}$ and $j_\gamma = l$ for $M_{l\pm}$. Here $W_R$ is the mass and $\Gamma$ the total width of the resonance; q and k are CM momenta of the kaon and photon, respectively. The phase angle $\delta_\infty$ is considered to be independent of total CM energy W. Also $\Gamma_{if}$ is defined by $\Gamma_{if} = \sqrt{\Gamma_{\gamma p}\Gamma_{KY}}$ where $\Gamma_{\gamma p}$ and $\Gamma_{KY}$ are the partial decay widths of the

resonance to the states $\gamma$p and $K^+\Lambda$ or $K^+\Sigma^0$; the electric and magnetic transitions are distinguished by $\Gamma^E_{if}$ $\Gamma^M_{if}$.

### 2.2.4 Quark Models

The subtlety and complexity of Quantum Chromodynamics (QCD) has so far prohibited analytic solutions which could be used in discussions of the non-perturbative aspects of the nucleon structure at any practical level. The nucleon as a condensate of strongly interacting quarks and gluons offers such a rich phenomenology that, despite massive numerical efforts in lattice QCD, for physical insights into many facets, models are still helpful. The isobaric model, where Feynman diagrammatic technique is used so that the transition amplitudes are Lorentz invariant, has no explicit connection with the QCD as meson baryon interactions are treated at the phenomenological level and number of parameters in these models are generally related to the number of resonances that are included in calculations. Thus it becomes necessary to investigate the reaction mechanism in terms of quark and gluon degrees-of-freedom.

#### Chiral Quark Model

As we know QCD is not solvable in a comprehensive manner at low and intermediate energies. There has been attempts to simulate QCD in these energy regions through the introduction of models of QCD. It is, however mandatory for them to satisfy the QCD properties. Quark models provide a promising approach to low-energy processes of hadrons and suitable to incorporate the relevant properties of QCD. Among them is undoubtedly the spontaneous breaking of Chiral symmetry as a fundamental dynamical principle. Chiral quark model is one such model that relies on those degrees-of-freedom that are brought about by spontaneous breaking of Chiral symmetry, namely constituent quarks and Goldstone bosons.

The strong interaction of the u,d,s quarks are described by the QCD Lagrangian

$$\mathcal{L} = i\bar{\psi}_L \not{D}\psi_L + i\bar{\psi}_R \not{D}\psi_R - \bar{\psi}_L M\psi R - \bar{\psi}_R M\psi_L, \tag{2.41}$$

where,

$$\psi_{L,R} = \begin{bmatrix} u \\ d \\ s \end{bmatrix} \tag{2.42}$$

$$D_\mu = \partial_\mu + igG_\mu \tag{2.43}$$

$$M = \begin{bmatrix} m_u & & \\ & m_d & \\ & & m_s \end{bmatrix} \tag{2.44}$$

In Eq.(2.43) g is the gluon coupling constant and $G_\mu$ is the gluon field. If we neglect the mass term, then $\mathcal{L}$ has an $SU(3)_L \otimes SU(3)_R$ chiral flavour symmetry. Introduction of mass leads to breakdown of chiral symmetry from $SU(3)_L \otimes SU(3)_R$. This implies that there must be an octet of Goldstone bosons: the $\pi$'s, K's and $\eta$. These pseudoscalar Goldstone boson fields are essential if the Lagrangian is to consistently reproduce the effects of a spontaneously broken global symmetry. The pseudoscalar Goldstone bosons can be represented in 3x3 matrix field $U(x) \in SU(3)$ with $U^\dagger U$=1. This matrix transforms linearly under the chiral rotations $\psi_R \rightarrow R\psi_R$ and $\psi_L \rightarrow L\psi_L$ of the right and left handed quarks to

$$U \rightarrow RUL^\dagger \tag{2.45}$$

The explicit representation of U in terms of the octet of pseudoscalar Goldstone boson fields, $\pi_a(x)$, is as follows:

$$U(x) = exp\left[\frac{i\phi(x)}{f}\right], \tag{2.46}$$

with

$$\phi \equiv \lambda_a \pi_a = \sqrt{2} \begin{pmatrix} \frac{\pi^0}{\sqrt{2}} + \frac{\eta}{\sqrt{6}} & \pi^+ & K^+ \\ \pi^- & \frac{-\pi^0}{\sqrt{2}} + \frac{\eta}{\sqrt{6}} & K^0 \\ K^- & K^0 & -2\frac{\eta}{\sqrt{6}} \end{pmatrix} \tag{2.47}$$

In the bag model vector current is quite satisfactory but axial current is a different matter. Assuming flavour $SU(2)$, with the quark field operator, $\psi$, a two component vector for up and down quarks, we consider the chiral transformation, under which the QCD Lagrangian is invariant

$$\psi \rightarrow \psi - \frac{i\boldsymbol{\tau} \cdot \boldsymbol{\epsilon}}{2}\gamma_5\psi, \tag{2.48}$$

$$\bar{\psi} \rightarrow \bar{\psi} - i\bar{\psi}\frac{\boldsymbol{\tau} \cdot \boldsymbol{\epsilon}}{2}\gamma_5. \tag{2.49}$$

For the bag, the surface term, $\frac{-1}{2}\bar{\psi}\psi\delta_s$, which is essential to confine the quarks, breaks the invariance under above chiral transformation. Instead of being conserved, the axial current

$$A^\mu = \bar{\psi}\gamma^\mu\gamma_5\frac{\boldsymbol{\tau}}{2}\psi\theta_v \tag{2.50}$$


Figure 2.3: Violation of chiral symmetry at the bag surface.

satifies

$$\partial_\mu A^\mu = -i\bar{\psi}\gamma_5 \frac{\tau}{2}\psi\delta_s. \tag{2.51}$$

The physical origin of this symmetry breaking is illustrated in the Fig.2.3.

Since the confinement implies that any quark impinging on the bag surface must be reflected and is provided by the Lorentz scalar interaction. However there is no spin-flip associated with the reflection and hence the chirality, or handedness, of the quark is changed. This violates chiral symmetry. Even within QCD itself the naive expectations based on chiral symmetry gets into trouble. The hadronic spectrum shows no degeneracy between positive and negative parity states and therefore the exact chiral symmetry of massless QCD must be dynamically broken leading to a vacuum containing massless Goldstone bosons - the pions in two flavour QCD. This realization rescues us from the problem we have just encountered and a large number of phenomenological models have been constructed on the basis of this solution. The idea is to add terms involving a pion field to the basic bag model Lagrangian density. This field should be coupled to the confined quarks in such a way that under a chiral transformation of both the quark and pion fields the new Lagrangian density is invariant and therefore yields a conserved axial current.

There are many choices possible for the Lagrangian density of such a chiral quark model. The following Lagrangian [58] has been the basis of an enormous amount of work, beginning in late 1970's:

$$\mathcal{L}_{CBM} = [i\bar{\psi}\gamma_\mu\partial^\mu\psi - B]\theta_v - \frac{1}{2}\bar{\psi}e^{\frac{i\tau\cdot\phi\gamma_5}{f}}\psi\delta_s + \frac{1}{2}(D_\mu\phi)^2. \tag{2.52}$$

Here covariant derivative on the pion field is:

$$D_\mu\phi = (\partial_\mu\phi)\hat{\phi} + f sin(\frac{\phi}{f})\partial_\mu\hat{\phi} \tag{2.53}$$

or,

$$= (\partial_\mu\phi + O(\phi^3) \tag{2.54}$$

where B is phenomenological energy density of bag, $\theta_v$ defines the bag volume and $\hat{\phi}$ is a unit vector in isospin space pointing in the direction of $\phi$. By construction the Lagrangian density is invariant under the chiral transformation:

$$\psi \rightarrow \psi - \frac{i\tau \cdot \epsilon}{2}\gamma_5\psi \tag{2.55}$$

$$\bar{\psi} \rightarrow \bar{\psi} - i\bar{\psi}\frac{\tau \cdot \epsilon}{2}\gamma_5 \tag{2.56}$$

$$\phi \rightarrow \phi + \epsilon f + f(\epsilon \times \hat{\phi}) \times \hat{\phi}\left[1 - \frac{\phi}{f}cot(\frac{\phi}{f})\right]. \tag{2.57}$$

As a consequence there is a conserved axial current $\mathbf{A}^\mu$, which has the form

$$\mathbf{A}^\mu = \bar{\psi}\gamma^\mu\gamma_5\frac{\tau}{2}\psi\theta_v + \left[f\hat{\phi}(\partial^\mu\phi) + \frac{f^2}{2}\partial^\mu\hat{\phi}sin(\frac{2\phi}{f})\right] \tag{2.58}$$

$$= \mathbf{A}^\mu_{\mathbf{quark}} + f\partial^\mu\phi + \mathcal{O}(\phi^3). \tag{2.59}$$

### Chiral Color Dielectric Model

Chiral model, like bag model suffer from several limitations. First, the use of an artificial bag to confine quarks leads to wavefunctions which have sharp discontinuities at the bag boundary. This leads to meson-baryon form factors and potentials containing unphysical oscillations and, presumably, limited ability to describe the scattering data. In addition, bag calculations treat the bare baryon masses and the bag radius as independent parameters which is not correct as for massless quarks the baryon masses are inversely proportional to the bag radius. The chiral color dielectric model(CCDM) [62] is a non-topological soliton model, which was first introduced to simulate phenomenologically the absolute color confinement of quantum chromodynamics (QCD). A connection with the more fundamental theory was established by Nielson and Patkos [59] who found that an effective color dielectric field does indeed arise naturally in lattice QCD after defining "coarse grained" effective field variables. The color dielectric field takes into account the long distance behaviour of the QCD vacuum and produces a natural confinement of the quarks within baryons. More recently, confinement and a pseudoscalar meson (Goldstone boson) have been found to arise naturally if chiral symmetry is dynamically broken. In some recent CCDMs, chiral symmetry is restored via a non-linear realization which introduces an elementary pion field as a Goldstone boson. Even though the mesons in these models are elementary, the baryon structure and the resulting relations of coupling constants are determined by the quark model [60, 61].

In application CCDM is similar to the chiral bag model (CBM) [58, 61] yet somewhat more microscopic in its dynamic mechanism for quark confinement and its treatment of baryon recoil within a nontopological-soliton solution to the field equations.

The Lagrangian density for the CCDM is given by [60, 62]:

$$\begin{aligned}\mathcal{L} &= \sum_f \bar{\psi}_f(x)\Big[i\gamma^\mu\partial_\mu - \frac{m_f}{\chi^p(x)}exp(\frac{i}{f_\phi}\gamma_5\tau\cdot\phi(x)) \\ &\quad -\frac{1}{2}g_s\lambda_a\gamma^\mu A^a_\mu(x)\Big]\psi_f(x) + \frac{1}{2}\sigma_v^2(\partial_\mu\chi(x))^2 - \frac{1}{4}\mathcal{K}(\chi)F^a_{\mu\nu}(x)F^{\mu\nu}_a(x) \\ &\quad -\frac{1}{2}m_\phi^2(\phi(x))^2 + \frac{(D_\mu\phi)^2}{2} - U(\chi) \qquad (2.60)\end{aligned}$$

where $\psi(x)$, $\chi(x)$, $\phi(x)$ and $A^\mu(x)$ are the effective quark , color dielectric, pseudoscalar meson and gluon fields respectively, $\lambda_a$are $SU(3)$ Gell Mann matrices, and f is the average weak decay constant of the pseudoscalar meson octet. Sum is over all color and flavour indices and $m_f$ is the flavour dependent effective quark mass, $m_\phi$ is the pseudoscalar meson mass and $F^a_{\mu\nu}(x)$ is the color electromagnetic field tensor:

$$F^a_{\mu\nu} = \partial_\mu A^a_\nu(x) - \partial_\nu A^a_\mu(x) - ig_s f^{abc}A^b_\mu(x)A^c_\nu(x). \qquad (2.61)$$

The effective gluon field interacts with the color dielectric field through a dielectric functional $\mathcal{K}(x) = \chi^f(x)$. The important part of Lagrangian (2.60) is the dielectric self interaction field $U(\chi)$ which accounts for average gluon field and produces a self consistent, dynamic confinement of the quarks, its form is

$$U(\chi) = B[\alpha\chi^2 - 2(\alpha-2)\chi^3 + (\alpha-3)\chi^4]. \qquad (2.62)$$

The potential $U(\chi)$ is such that if $\alpha > 6$, it has a double well structure with an absolute minimum at $\chi$=0 and a secondary minimum at $\chi$=1. These can be identified with the physical and perturbative vaccua of QCD respectively. The energy density difference between two minima measures the pressure of the physical vacuum, i.e. bag constant B. (Fig.2.4).

The curvature at $\chi$ =0 is related to the scalar field mass

$$m_{GB} = \sqrt{\frac{2B_\alpha}{\sigma_v^2}}.$$

Thus one can consider $m_{GB}$(glueball mass) instead of $\sigma_v$ as an independent parameter.

The behaviour of Lagrangian Eq.(2.60) is of particular importance in the limit of vanishing dielectric field, $\chi \to 0$. In this limit the gluon kinetic energy term $\chi^4\frac{F^2}{4}$

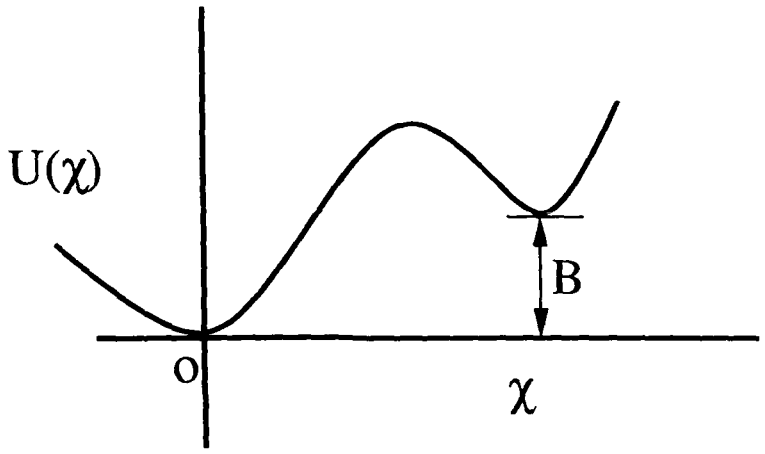


Figure 2.4: Plot of $U(\chi)$ vs $\chi$

vanishes and quark effective mass $\frac{m_f}{\chi}$ becomes infinite. Accordingly we have the distinguishing characteristic of CCDM: The quark gluon fields are confined within the baryon to the region of non-vanishing dielectric field $\chi$, whereas in bag model confinement is externally imposed placing the quarks within an infinite square well.

# Chapter 3

# Form Factors and Amplitude Calculation

Most photoproduction calculations in the energy region near threshold ($E_\gamma$=0.911 GeV) are variations of a phenomenological model which treats the baryons as structureless elementary particles [5, 11, 66], that is with no form factors . These models include a large number of resonances with no resonance appearing to dominate, making calculations very complex and number of parameters needing adjustment keeps on increasing. When applied to hypernuclear photoproduction these models are useful and provide excellent fits to the data, but their relation to the elementary strong interactions is not clear.

It has ben determined experimentally that hadrons have spatial extension and therefore can not be described as point particles. Hence, the possible reason for discrepancy between electromagnetic and hadronic coupling constants derived from the study of kaon photoproduction $\gamma p \rightarrow K^+ \Lambda$ and kaon scattering and $SU_F(3)$, respectively may be due to excluding the composite nature of hadrons in electromagnetic calculations. Accordingly, the Feynman diagrams which have only coupling constants at the hadronic vertices need to be generalized to include form factors, depicting the composite nature of the particles.

The cross-section for scattering due to an extended target, e.g. due to a particle

with charge density $\rho$(r), may be written as

$$(\frac{d\sigma}{d\Omega}) = (\frac{d\sigma}{d\Omega})_{point}|F(q^2)|^2 \tag{3.1}$$

here q is the momentum transfer and $(\frac{d\sigma}{d\Omega})_{point}$ is the cross-section due to a point particle. The form factor may be defined as the ratio between the amplitude of scattering by an extended charge distribution and a point scatterer. For a static target $F(q^2)$ is simply the Fourier transform of the charge distribution $\rho(\mathbf{r})$

$$F(q^2) = \int \rho(\mathbf{r}) e^{i\mathbf{q}.\mathbf{r}} d^3r. \tag{3.2}$$

If $\rho(\mathbf{r})$ is spherically symmetric $F(q^2)$ is a function only of the magnitude $|\mathbf{q}|$. For a point particle, $\rho(\mathbf{r})=\delta(\mathbf{r})$, so that $F(q^2)=1$.

The form factors are useful and essential quantities for many reasons. These have bearing on the underlying structure of hadrons as in perturbative chiral quark models [67] the pion-baryon form factors are directly related to the quark wave functions in baryons. Form factors are essential in the effective models of meson-baryon, interaction, as hadrons are not point particles. For a consistent description of nuclear phenomena one also needs these from factors. The phenomenological vertex form factors related to the structure of hadrons, are included in meson-exchange nucleon-nucleon potentials. Form factors are also needed in computation of photoproduction and electroproduction of baryon resonances as photon can couple to the virtual charged meson cloud in a baryon. The technical utility of form factors is to provide necessary cut-off functions in effective meson-baryon interaction models, which are generally not renormalizable.

The Feynman diagrams contributing to kaon photoproduction $\gamma p \rightarrow K^+ \Lambda$ are given in Fig.3.1.

The lowest order (tree level) scattering amplitude for the photon-kaon production can be described by the absorption of the photon on the proton followed by the emmission of kaon (the pole term) and the associated crossed diagram (Fig.3.1(a) and 3.1(b)) repspectively. The baryon in the intermediate state can be in an excited state of the nucleon (resonance) depending on the energy of photon. But here we are excluding the resonances in the intermediate state. In addition to pole and crossed terms, two more diagrams contribute at tree level. These are the seagull term (Fig.3.1(c)) (if the kaon-quark coupling is of derivative type) and the direct reaction type diagram (Fig.3.1(d)) involving $\gamma K^+$ $K^+$ vertices. The calculation requires the coupling of photon and kaon with baryons. This means that photon and kaon interaction is expressed in terms of

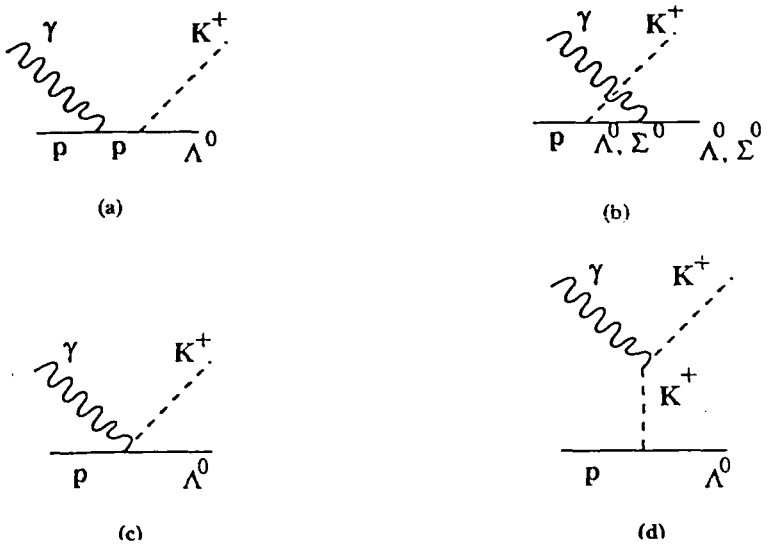


Figure 3.1: Tree level diagrams contributing to kaon photoproduction

coupling parameters and form factors associated with them. These could be considered as phenomenological parameters used to fit the data or obtained from other reactions. On the other hand, one may attempt to derive them from a model of baryons. Here we have used quark model to compute these.

## 3.1 Form Factors at Quark Level

In our calculations, the form factors are determined from a quark model of hadrons and the interaction of photons and kaons with the quarks. The interaction Lagrangian for quark-kaon interaction is

$$\mathcal{L}_I^Q = \frac{1}{2f}\overline{\psi}_q \gamma^\mu \gamma_5 \lambda_a . \partial_\mu \phi_a \psi_q \tag{3.3}$$

where, $\phi_a$ is the pseudoscalar kaon field operator with SU(3) flavour index a, f is the decay constant which is same as pion decay constant, $\lambda_a$ are Gell-Mann matrices and $\psi_q$ is the quark wave function , which is written in the following form

$$\psi_q = \psi(\mathrm{r})\zeta = \begin{pmatrix} g(r) \\ i(\sigma.\hat{r})f(r) \end{pmatrix} \zeta \tag{3.4}$$

where $\zeta$ contains flavour and spin wave functions

$$\zeta = \chi_{flavour}\chi_{spin}. \tag{3.5}$$

The function g(r) and f(r) represent upper and lower components of the Dirac spinor $\psi_q(\mathbf{r})$.

Using the form of $\psi_q$ in Eq.(3.3) we get for $pK^+\ \Lambda$ vertex

$$\mathcal{L}_I^Q = \frac{1}{2f}\langle \chi^{\Lambda}_{flavour}\chi^{\Lambda}_{spin}|\overline{\psi}(\mathbf{r})\gamma^{\mu}\gamma_5\lambda_{\mathbf{a}}.\partial_{\mu}\phi_a\psi_{(\mathbf{r})}|\chi^{p}_{flavour}\chi^{p}_{spin}\rangle. \tag{3.6}$$

Let us consider first the product $\overline{\psi}(\mathbf{r})\gamma^{\mu}\gamma_5\lambda_{\mathbf{a}}.\partial_{\mu}\phi_{\mathbf{a}}\psi_{(\mathbf{r})}$ which on simplifying reduces to

$$i(g_s(r), -i(\boldsymbol{\sigma}.\hat{r})f_s(r))\gamma^0(\gamma^0 q_0 - \boldsymbol{\gamma}.\mathbf{q})\gamma_5 \begin{pmatrix} g_u(r) \\ i(\boldsymbol{\sigma}.\hat{r})f_u(r) \end{pmatrix} \lambda_{\mathbf{a}} \tag{3.7}$$

where s and u notation is for s-quark and u-quark. $\lambda_a$ operates only on spin flavour part. Here we consider only $\boldsymbol{\gamma}\cdot\mathbf{q}$ product as $\gamma^0 q_0$ term vanishes, where $q_\mu$ is the four-momentum of kaon. Thus we have

$$-i(g_s(r), -i(\boldsymbol{\sigma}.\hat{r})f_s(r))\gamma^0\boldsymbol{\gamma}.\mathbf{q}\gamma_5 \begin{pmatrix} g_u(r) \\ i(\boldsymbol{\sigma}.\hat{r})f_u(r) \end{pmatrix} \lambda_{\mathbf{a}} \tag{3.8}$$

solving which we get

$$-i\left[\boldsymbol{\sigma}\cdot\mathbf{q}(g_s(r)g_u(r) - f_s(r)f_u(r)) + 2(\boldsymbol{\sigma}\cdot\mathbf{r})(\mathbf{q}\cdot\hat{r})f_s(r)f_u(r))\right]\lambda_a. \tag{3.9}$$

To get the form factor we have to take Fourier transform and integrate over $d^3r$. Taking first the term

$$-2if_s(r)f_u(r)\int(\boldsymbol{\sigma}.\hat{r})(\mathbf{q}.\hat{r})e^{i\mathbf{q}\cdot\mathbf{r}}d^3r$$

using

$$e^{i\mathbf{q}\cdot\mathbf{r}} = 4\pi\Sigma_{L,M}i^L j_L(qr)Y^*_{L,M}(q)Y_{L,M}(\mathbf{r}) \tag{3.10}$$

we obtain

$$-2if_s(r)f_u(r)4\pi\int(\boldsymbol{\sigma}\cdot\hat{r})(\mathbf{q}\cdot\hat{r})\Sigma_{L,M}i^L j_L(qr)Y^*_{L,M}(q)Y_{L,M}(\mathbf{r}). \tag{3.11}$$

Using the identity

$(\mathbf{A}\cdot\mathbf{C})(\mathbf{B}\cdot\mathbf{D}) = \frac{1}{3}(\mathbf{A}\cdot\mathbf{B})(\mathbf{C}\cdot\mathbf{D}) + \frac{1}{2}(\mathbf{A}\times\mathbf{B})(\mathbf{C}\times\mathbf{D}) + T_2(\mathbf{A},\mathbf{B}).T_2(\mathbf{C},\mathbf{D})$ we can simplify the

$(\boldsymbol{\sigma}.\hat{r})(\mathbf{q}\cdot\hat{r}) = \frac{1}{3}(\boldsymbol{\sigma}\cdot\mathbf{q})(\hat{r}\cdot\hat{r}) + \frac{1}{2}(\boldsymbol{\sigma}\times\mathbf{q})(\hat{r}\times\hat{r}) + T_2(\boldsymbol{\sigma},\mathbf{q}).T_2(\hat{r},\hat{r})$ where $T_2$ indicates the tensor product of rank two.

Simplifying further we get

$(\boldsymbol{\sigma}\cdot\hat{r})(\mathbf{q}.\hat{r}) = \frac{1}{3}(\boldsymbol{\sigma}\cdot\mathbf{q})(\hat{r}\cdot\hat{r}) + \Sigma_m T_{2m}(\boldsymbol{\sigma},\mathbf{q}).Y^*_{2m}(\hat{r})$. Using this expression in Eq.(3.11) we obtain

$$-i4\pi \int \left[\frac{1}{3}(\boldsymbol{\sigma}\cdot\mathbf{q})\Sigma_{L,M} i^L j_L(qr) Y_{L,M}(q) Y^*_{L,M}(\hat{r}) + \Sigma_m T_{2m}(\boldsymbol{\sigma},\mathbf{q}) Y^*_{2m}(\hat{r})\right.$$

$$\left.\Sigma_{L,M} i^L j_L(qr) Y_{L,M}(q) Y^*_{L,M}(\hat{r})\right] 2 f_s(r) f_u(r) r^2 dr d\Omega. \tag{3.12}$$

Now

$$Y^*_{2m}(\hat{r}) Y_{L,M}(q) = \delta_{2L}\delta_{mM} \text{ and } \hat{r} = \mathbf{q}$$

which gives

$$T_2(\boldsymbol{\sigma},\mathbf{q}).T_2(\hat{r},\hat{r}) = T_2(\boldsymbol{\sigma},\mathbf{q}).T_2(\mathbf{q},\mathbf{q}) = \frac{2}{3}\sigma\cdot\mathbf{q}. \tag{3.13}$$

Therefore we have from Eq.(3.12)

$$-i4\pi\left[\frac{1}{3}(\boldsymbol{\sigma}\cdot\mathbf{q})\int j_0(qr) + \frac{2}{3}(\boldsymbol{\sigma}\cdot\mathbf{q})\int j_2(qr)\right] 2 f_s(r) f_u(r) r^2 dr. \tag{3.14}$$

Similarly for

$$(\boldsymbol{\sigma}\cdot\mathbf{q})\left[g_s(r)g_u(r) - f_s(r)f_u(r)\right]\int e^{i\mathbf{q}\cdot\mathbf{r}} d^3r$$

we obtain

$$4\pi(\boldsymbol{\sigma}\cdot\mathbf{q})\int j_0(qr)\left[g_s(r)g_u(r) - f_s(r)f_u(r)\right] r^2 dr. \tag{3.15}$$

Combining these two Eqs.(3.14 and 3.15) we obtain

$$4\pi\left\{(\boldsymbol{\sigma}\cdot\mathbf{q})\int j_0(qr)\left[g_s(r)g_u(r) - \frac{1}{3}f_s(r)f_u(r)\right] + \frac{4}{3}\int j_2(qr) f_s(r) f_u(r)\right\} r^2 dr. \tag{3.16}$$

Now there remains to solve the spin flavour part i.e.

$$\langle \chi^{\Lambda}_{spin}\chi^{\Lambda}_{flavour} | \sigma_z.\lambda_a | \chi^{p}_{spin}\chi^{p}_{flavour}\rangle \tag{3.17}$$

$\sigma_z$ operates on third quark (here u quark) and due to symmetry we use only $\sigma_z$. $\lambda_a$ changes u-quark to s-quark. The suitable combination for $\lambda_a$ in terms of Gell-Mann matrices is

$$\left(\frac{\lambda_4 - i\lambda_5)}{2}\right. \tag{3.18}$$

where

$$\lambda_4 = \begin{pmatrix} 0 & 0 & 1 \\ 0 & 0 & 0 \\ 1 & 0 & 0 \end{pmatrix}, \lambda_5 = \begin{pmatrix} 0 & 0 & -i \\ 0 & 0 & 0 \\ -i & 0 & 0 \end{pmatrix} \tag{3.19}$$

$$\frac{1}{2}(\lambda_4 - i\lambda_5)u = \begin{pmatrix} 0 & 0 & 0 \\ 0 & 0 & 0 \\ 1 & 0 & 0 \end{pmatrix} \begin{pmatrix} 1 \\ 0 \\ 0 \end{pmatrix} = \begin{pmatrix} 0 \\ 0 \\ 1 \end{pmatrix} \equiv s, \tag{3.20}$$

which is the wavefunction for s-quark.

Using wavefunction for $\Lambda^0$ and p in Eq.(3.17) we obtain

$$\frac{1}{\sqrt{2}}\langle(\phi_{MS}\chi_{MS} + \phi_{MA}\chi_{MA})|\sigma_z(\frac{\Lambda_4 - i\Lambda_5}{2})|\frac{1}{\sqrt{2}}(\phi_{MS}\chi_{MS} + \phi_{MA}\chi_{MA})\rangle \tag{3.21}$$

which on solving further provides a factor of $\frac{1}{\sqrt{6}}$ , which when further multiplied by 3 (number of quarks) gives a factor of $\frac{\sqrt{3}}{2}$. Therefore our final expression is

$$-\frac{1}{2f}\frac{\sqrt{3}}{2}4\pi(\sigma \cdot \mathrm{q})\left[\int j_0(qr)(g_s(r)g_u(r) - \frac{1}{3}f_s(r)f_u(r)) + \frac{4}{3}\int j_2(qr)f_s(r)f_u(r)\right]r^2dr. \tag{3.22}$$

To find out the vertex form factors for gamma coupling with p and $\Lambda^0$ ($\Sigma^0$) i.e. at vertex $\gamma$pp and $\gamma$ $\Lambda\Lambda(\Sigma^0\Sigma^0)$, in case of Fig.3.1(a) and Fig.3.1(b), we use the interaction Lagrangian as

$$\mathcal{L}_I^Q = e\bar{\psi}_q\gamma^\mu A_\mu\psi_q. \tag{3.23}$$

Let us consider first the vertex $\gamma$pp, where gamma couples with the u quark of proton . Hence, $e = \frac{2}{3}$Q. In Eq.(3.23) $\psi_q$ is same as in Eq.(3.4) and $A_\mu$ is the photon field. Substituting the form of $\psi_q$ in Eq.(3.23) we may write:

$$\mathcal{L}_I^Q = \frac{2}{3}[g_u(r), -i(\sigma \cdot \hat{r})f_u(r)]\,\gamma^0(\gamma^0\epsilon_0 - \gamma \cdot \epsilon)\gamma_5 \begin{pmatrix} g_u(r) \\ i(\sigma.\hat{r})f_u(r))\lambda_a. \end{pmatrix}. \tag{3.24}$$

Where the terms involved are already defined. For real photon $\epsilon_0$=0; hence we obtain from Eq.(3.24) upon solving further

$$\mathcal{L}_I^Q = \frac{4}{3}\sigma.(\epsilon \times \mathrm{r})f_u(r)g_u(r). \tag{3.25}$$

Now, since there are three quarks involved and by symmetry we have taken only third quark above. Thus Eq.(3.25) must be multiplied by 3, also a factor of 1 comes due to spin-flavour part of wavefunction. We obtain

$$\mathcal{L}_I^Q = 4\sigma.(\epsilon \times \mathrm{r})f_u(r)g_u(r). \tag{3.26}$$

For $\gamma\Lambda^0\Lambda^0(\Sigma^0\Sigma^0)$ vertex where $\gamma$ couples with s quark the Eq.(3.25) is written as

$$\mathcal{L}_I^Q = -\frac{2}{3}\sigma.(\epsilon \times \mathbf{r}) f_s(r) g_s(r), \tag{3.27}$$

where factor of $-\frac{1}{3}$ is included which comes from spin-flavour part of wave function.

The form factor to be determined is just the Fourier transform of the charge distribution. Taking Fourier transform of Eq.(3.26) we have

$$4\int e^{i\mathbf{k}\cdot\mathbf{r}}\sigma \cdot (\epsilon \times \mathbf{r}) f_u(r) g_u(r) r^2 dr d\Omega, \tag{3.28}$$

solving which we get

$$i16\pi(\epsilon \times \sigma).\frac{\mathbf{k}}{k}\frac{\partial}{\partial k}\int \frac{f_u(r)g_u(r)}{r}\frac{sinkr}{kr}r^2 dr, \tag{3.29}$$

and similarly for $\gamma\Lambda^0\Lambda^0(\Sigma^0\Sigma^0)$ vertex we obtain from Eq.(3.27)

$$-i\frac{8}{3}\pi(\epsilon \times \sigma).\frac{\mathbf{k}}{k}\frac{\partial}{\partial k}\int \frac{f_s(r)g_s(r)}{r}\frac{sinkr}{kr}r^2 dr. \tag{3.30}$$

## 3.2 Form Factors at Nucleon Level

To realize the importance of form factors at nucleon level, we have to switch back over to nucleons from quarks and obtain the form factors at nucleon level using non-relativistic limit. The coupling of gamma with proton is given by the expression

$$\overline{\psi}\left[\gamma^\mu A_\mu F_1(k^2) + \frac{1}{2M}\chi_N F_2(k^2)\sigma^{\mu\nu}\partial_\mu A_\nu\right]\psi, \tag{3.31}$$

where $\psi$ is the nucleonic wave function, $A_\mu$ the photon field, $F_1$ and $F_2$ the charge and magnetic form factors, repectively , $\chi_N$ the anamolous magnetic moment of proton and $\sigma^{\mu\nu}$ the tensor operator.

In non-relativistic limit Dirac spinor

$$\psi = \sqrt{\frac{E+M}{2M}}\begin{pmatrix} 1 \\ \frac{\sigma\cdot\mathbf{p}}{E+M} \end{pmatrix} \tag{3.32}$$

reduces to

$$\psi = \begin{pmatrix} 1 \\ \frac{\sigma\cdot\mathbf{p}}{E+M} \end{pmatrix}. \tag{3.33}$$

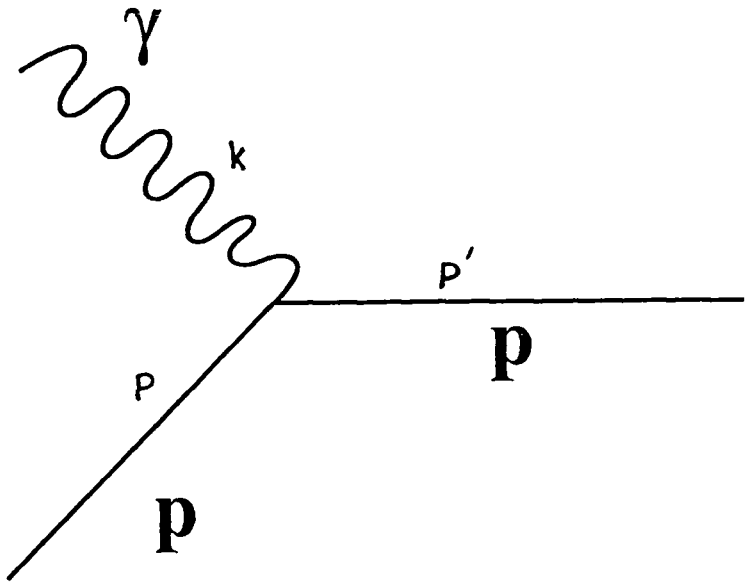


Figure 3.2: $\gamma$pp vertex.

Along with non-relativistic limit we use brick wall frame, where $\mathbf{p}'$, the momentum of intermediate proton is equal to -p, the momentum of proton , as shown in Fig.3.2

From Fig. 3.2 we can see that $\mathbf{p}' - \mathbf{p} = \mathbf{k}$, which gives $\mathbf{p}' = \frac{\mathbf{k}}{2}$ and $\mathbf{p} = -\frac{\mathbf{k}}{2}$. Where $\mathbf{k}$ is the momentum of photon.

Using Eq.(3.33) and values of $\mathbf{p}'$ and $\mathbf{p}$ in Eq.(3.31) we get

$$-i\frac{\mathbf{k}\cdot(\epsilon\times\sigma)}{2M}[F_1(0)+\chi_N F_2(0)], \tag{3.34}$$

on comparing it with Eq.(3.29) we obtain

$$\frac{1}{2M}[F_1(0)+\chi_N F_2(0)] = 16\pi\frac{1}{k}\frac{\partial}{\partial k}\int\frac{f_u(r)g_u(r)}{r}\frac{sinkr}{kr}r^2dr. \tag{3.35}$$

The form factor for $\gamma\Lambda^0\Lambda^0(\Sigma^0\Sigma^0)$ vertex (Fig.3.3) is determined, by using the expression

$$\frac{1}{2M}\overline{\psi}[\chi_N F_2(k^2)\sigma^{\mu\nu}\partial_\mu A_\nu]\psi, \tag{3.36}$$

where the terms involved are already defined. For $\Lambda^0$ $\gamma^\mu A_\mu F_1(k^2)$=0, due to its neutral charge. Solving Eq.(3.36) by using non-relativistic limit and brick wall frame (Fig.3.3) and then comparing it with Eq.(3.30)we get

$$\frac{\chi_N}{2M}F_2(0) = -8\pi\frac{1}{k}\frac{\partial}{\partial k}\int\frac{f_s(r)g_s(r)}{r}\frac{sinkr}{kr}r^2dr. \tag{3.37}$$

Next we have to compare the form factor obtained at $pK^+\Lambda^0$ vertex (Fig.3.4) with the one obtained when $K^+$ couples with u-quark of proton. From Fig.3.4 we can see that

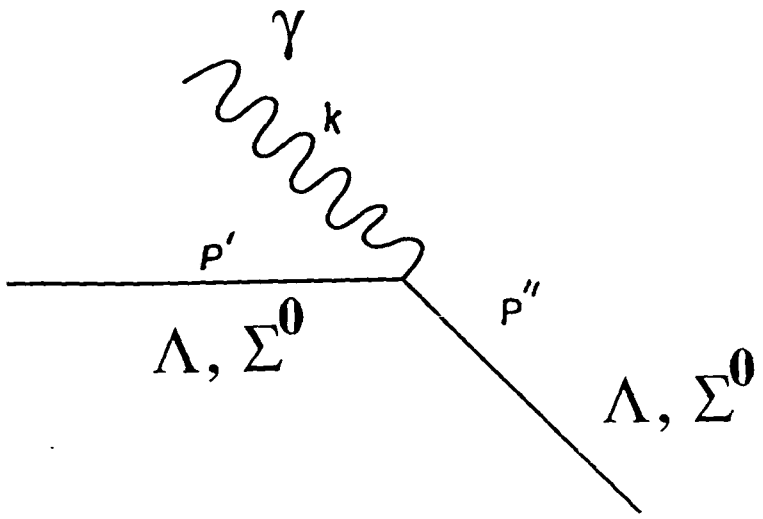


Figure 3.3: $\gamma\Lambda^0\Lambda^0(\Sigma^0\Sigma^0)$ vertex.

$\mathbf{p'} = \mathbf{q} + \mathbf{p''}$, where $\mathbf{p'}$, $\mathbf{q}$ and $\mathbf{p''}$, is the momentum of proton , kaon and Lambda respectively. Further We can write $pK^+\Lambda^0$ vertex as

$$\overline{\psi}_{\Lambda^0}\gamma^\mu\gamma_5 F_\phi(q^2)\psi_p, \tag{3.38}$$

where $\psi_{p,\Lambda^0}$ is the wave function for proton and $\Lambda^0$ repectively and $F_\phi(q^2)$ is form factor at $pK^+\Lambda^0$ vertex.

Solving Eq.(3.38) using non-relativistic limit and brick wall frame and later on comparing with Eq.(3.22) we obtain

$$\begin{aligned} F_\phi(q^2) &= -i\frac{\sqrt{2}}{4}\pi\left\{\int j_0(qr)\left[g_s(r)g_u(r) - \frac{1}{3}f_s(r)f_u(r)\right]\right. \\ &\quad \left. + \frac{4}{3}\int j_2(qr)f_s(r)f_u(r)\right\} r^2 dr \end{aligned} \tag{3.39}$$

which is $K^+$ form factor at $pK^+\Lambda^0$ vertex i.e. $F_\phi(q^2) = F_{pK^+\Lambda}$.

The Eqs.( 3.35, 3.37 and 3.39) are plotted as a function of momentum transfer in Fig.(3.5). Where open circles connected with the solid line represent the plot of form factor for the coupling of $K^+$ with the proton (Eq.3.39). The plot of the form factor when photon couples with proton (Eq.3.35) is represented by the open squares connected with teh solid line. The plot with open triangles connected with the solid line represent the form factor for the coupling of photon with lambda. From the plot we can see that at q=0 the form factor at $pK^+\Lambda$ vertex is not zero but gives some finite value which may be said to be the coupling constant at $pK^+\Lambda$ vertex. But this

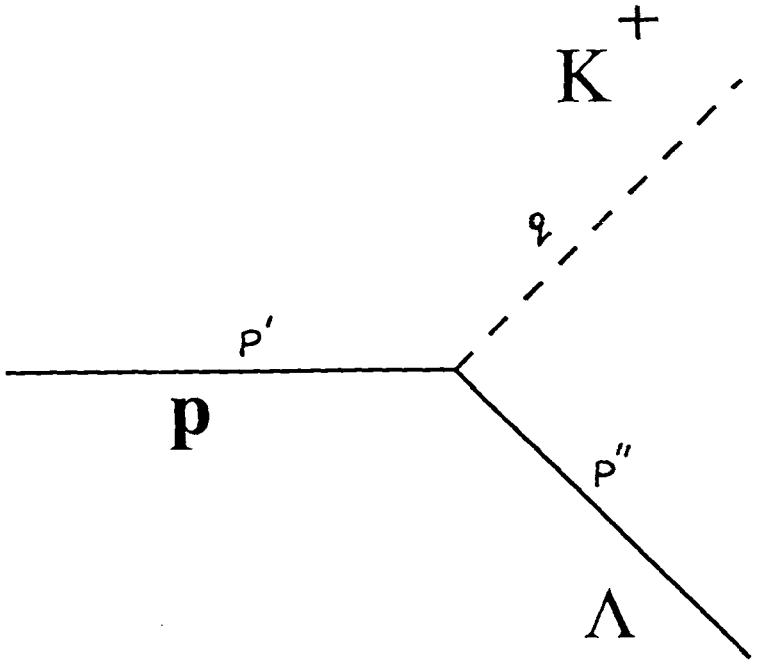


Figure 3.4: $pK^+\Lambda^0$ vertex.

is not the case with the form factors at two gamma vertices i.e. $\gamma pp$ and $\gamma\Lambda\Lambda$, which reduce to almost 0 value at q=0. Thus it may be said to provide magnetic moment. Near the value q=1200 MeV it can be seen that all the three form factors coincide and therefrom remain constant with the value of q.

## 3.3 Effective Lagrangians and Amplitudes

The effective Lagrangians for all the vertices of the Fig.3.1 are written down here and amplitudes for the elementary process $\gamma$+p$\rightarrow$K$^+\Lambda$ corresponding to Fig.3.1 are formulated in terms of CGLN amplitudes.

The effective Lagrangian for the kaon vertex is written as:

$$\mathcal{L}_{pK^+\Lambda} = \frac{F_{pK^+\Lambda}}{f}\overline{\psi}_\Lambda(\mathrm{p}')\gamma^\mu\gamma_5\partial_\mu\phi.\tau\psi_p(\mathrm{p}) \tag{3.40}$$

where p and p$'$ are momenta of proton and lambda, f is the decay constant whose value is 93 MeV equal to pion decay constant. The quantity $F_{pK^+\Lambda}$ is the quark model form factor multiplied by the coupling constant.

The Lagrangian for the photon vertices ,that is, pp$\gamma$ vertex may be written down

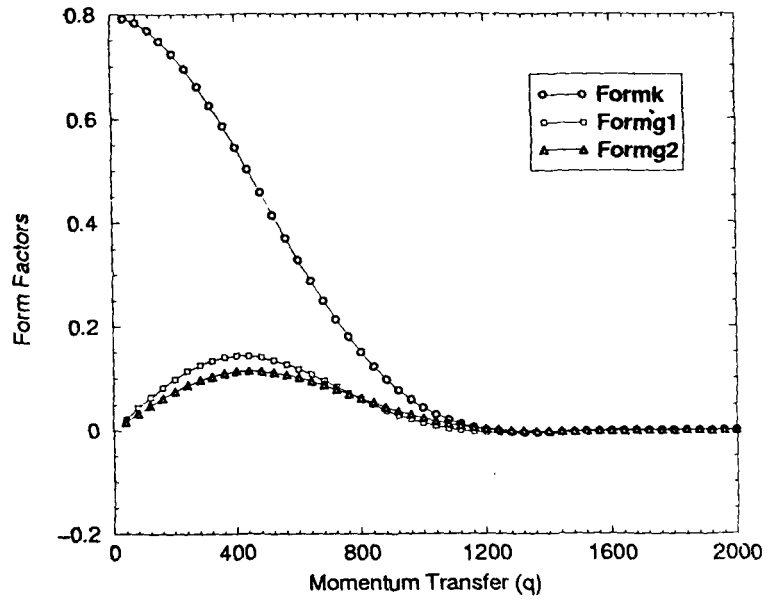


Figure 3.5: plot of Form Factors vs Momentum Transfer

as:

$$\mathcal{L}_{pp\gamma} = \overline{\psi}_p(\mathbf{p}') \left[ \gamma^\mu A_\mu F_1(k^2) + \frac{\chi_N}{2m_p} \sigma^{\mu\nu} F_2(k^2) \partial_\nu A_\mu \right] \psi_p(\mathbf{p}) \tag{3.41}$$

where $\mathbf{p}$ and $\mathbf{p}'$ are momenta of incoming proton and outgoing proton. The first part in the braces describe the electrical interaction of proton with photon and second part represents the magnetic part of interaction. $F_1(k^2)$ and $F_2(k^2)$ are the respective form factors. $\chi_N$ stands for the magnetic moment of proton.

The $\Lambda\Lambda\gamma$ vertex Lagrangian is:

$$\mathcal{L}_{\Lambda\Lambda\gamma} = F_{\Lambda\Lambda\gamma} \overline{\psi}_p(\mathbf{p}') \left[ \frac{\chi_N}{2m_\Lambda} \sigma^{\mu\nu} \partial_\nu A_\mu \right] \psi_\Lambda(\mathbf{p}) \tag{3.42}$$

where $\mathbf{p}$ and $\mathbf{p}'$ are momenta of incoming lambda and outgoing lambda. Unlike proton lambda has got no electrical interaction part as its charge is zero. $F_{\Lambda\Lambda\gamma}$ is the form factor at lambda lambda gamma vertex, whose form is given in Eq.(3.30).

For the joint photon-kaon seagull vertex, Lagrangian is

$$\mathcal{L}_{p\Lambda K^+\gamma} = ie \frac{F_{p\Lambda\Lambda K^+\gamma}}{f} \overline{\psi}_\Lambda(\mathbf{p}') \gamma^\mu \gamma_5 A_\mu \phi \cdot \tau \psi_p(\mathbf{p}) \tag{3.43}$$

$F_{p\Lambda\Lambda K^+\gamma}$ is the form factor at $p\Lambda K^+$ $\gamma$ vertex.

The Lagrangian for $\gamma K^+K^+$ vertex is

$$\mathcal{L}_{K^+K^+\gamma} = ieA^\nu \phi \partial_\nu \phi \tag{3.44}$$

which describes the interaction where $K^+$ is emitted first which on interacting with photon gives final $K^+$.

### 3.3.1 The CGLN Amplitudes

In the $K^+$-$\Lambda$ centre of mass frame, the momenta of incoming photon, outgoing kaon, incoming proton and outgoing lambda is given by $\mathbf{k}$, $\mathbf{q}$, $\mathbf{p'}$=-$\mathbf{k}$ and $\mathbf{p''}$=-$\mathbf{q}$, respectively. Using these definitions one obtains momentum $\mathbf{p'}$ of the intermediate baryon and hyperon propagators of the Fig.(3.1) using momentum conservation law.
The standard form of the CGLN [37] amplitude for the photoproduction reads as

$$\begin{aligned} \mathcal{M} &= \mathcal{M}_1 + \mathcal{M}_2 + \mathcal{M}_3 + \mathcal{M}_4 \\ &= i\boldsymbol{\sigma}\cdot\boldsymbol{\epsilon}F_1 + \boldsymbol{\sigma}\cdot\hat{q}\,(\boldsymbol{\sigma}\times\hat{k})\cdot\boldsymbol{\epsilon}F_2 + i\hat{q}\,(\boldsymbol{\sigma}\cdot\hat{k})\cdot\boldsymbol{\epsilon}F_3 \\ &\quad + i\hat{q}\,(\boldsymbol{\sigma}\cdot\hat{q})\cdot\boldsymbol{\epsilon}F_4 \end{aligned} \tag{3.45}$$

For kaon photoproduction, the CGLN amplitude may be decomposed diagramwise (Fig.3.1) as under:

$$\begin{aligned} F_1 &= F_1(a) + F_1(b) + F_1(c) + F_1(d) \\ F_2 &= F_2(a) + F_2(b) + F_2(c) + F_2(d) \\ F_3 &= F_3(a) + F_3(b) + F_3(c) + F_3(d) \\ F_4 &= F_4(a) + F_4(b) + F_4(c) + F_4(d) \end{aligned} \tag{3.46}$$

For the diagram(3.1a), we consider proton as an intermediate state after the photon is absorbed and a kaon is emitted. In the $K^+$ $\Lambda$ CM frame the momentum $\mathbf{p'}$ of this intermediate state is 0. The amplitude has the form

$$\begin{aligned} \mathcal{M}_1(a) &= \frac{F_{pK^+\Lambda}}{f}\overline{\psi}_\Lambda(\mathbf{p''})\gamma^\mu\gamma_5\partial_\mu\phi\psi(\mathbf{p'})\overline{\psi}(\mathbf{p}) \\ &\quad \left[\gamma^\mu A_\mu F_i(k^2) + \frac{\chi_N}{2m_p}\sigma^{\mu\nu}\partial_\nu A_\mu F_2(k^2)\right]\psi(\mathbf{p}) \end{aligned} \tag{3.47}$$

the form of the nucleon(proton) propagator is

$$\mathcal{P}_N(\mathbf{p'}) = \psi(\mathbf{p'})\overline{\psi}(\mathbf{p}) = \frac{\gamma^0 E' + \boldsymbol{\gamma}.\boldsymbol{p'} + m_p}{p_0'^2 - m_p^2}. \tag{3.48}$$

The amplitude, may be simplified in the CGLN form as

$$
\begin{aligned}
F_1(a) &= i\frac{F_{pK+\Lambda}}{p_0'^2-m_p^2}\sqrt{\frac{(E''+m_\Lambda)}{2m_\Lambda}\frac{(E+m_p)}{2m_p}}C^{\tau_\Lambda,\tau_K,\tau_p}_{m_{\tau_\Lambda},m_{\tau_K},m_{\tau_\Lambda}+m_{\tau_K}} \\
&\left(q_0+\frac{q^2}{E''+m_\Lambda}\right)\ (p_0'-m_p)\left[k_0\frac{\chi_N}{2m_p}F_2(k^2)-F_1(k^2)\right] \\
&+\ \frac{\chi_N}{2m_p}\frac{k^2}{E+m_p}F_2(k^2)(p_0'-m_p)\left(q_0+\frac{q^2}{E''+m_\Lambda}\right) \qquad (3.49)
\end{aligned}
$$

$$
\begin{aligned}
F_2(a) &= -\frac{F_{pK+\Lambda}}{p_0'^2-m_p^2}\sqrt{\frac{(E''+m_\Lambda)}{2m_\Lambda}\frac{(E+m_p)}{2m_p}}C^{\tau_\Lambda,\tau_K,\tau_p}_{m_{\tau_\Lambda},m_{\tau_K},m_{\tau_\Lambda}+m_{\tau_K}} \\
&\left(1+\frac{q_0}{E''+m_\Lambda}\right)\left(\frac{1}{E+m_p}\right)\left[k_0\frac{\chi_N}{2m_p}F_2(k^2)+F_1(k^2)\right] \\
&\frac{\chi_N}{2m_p}\left(\frac{q_0}{E''+m_\Lambda}+1\right)F_2(k^2)\,(p_0'+m_p) \qquad (3.50)
\end{aligned}
$$

$$F_3(1a)=0 \qquad (3.51)$$

$$F_4(a)=0. \qquad (3.52)$$

Thus we may write amplitude for Fig.(3.1a) as:

$$\mathcal{M}_1(a)=i\boldsymbol{\sigma}\cdot\epsilon F_1(a)+\boldsymbol{\sigma}\cdot\hat{q}(\boldsymbol{\sigma}\times\hat{k})\cdot\epsilon F_2(a). \qquad (3.53)$$

For the Fig.(3.1b), the momentum of the intermediate field $\Lambda$ is $\mathbf{p'}=-(\mathbf{q}+\mathbf{k})$ and energy $E'=\sqrt{m_p^2+k^2}-\sqrt{m_{K+}^2+q^2}$.
Therefore for spin-1/2 intermediate lambda field, the amplitude in general form reads as:

$$
\begin{aligned}
\mathcal{M}_1(b) &= \frac{F_{pK+\Lambda}}{f}\overline{\psi}_\Lambda(\mathbf{p''})\left[\frac{\chi_L}{2m_\Lambda}\sigma^{\mu\nu}\partial_\nu A_\mu F_2(k^2)\right] \\
&\psi(\mathbf{p'})\overline{\psi}(\mathbf{p'})\gamma^\mu\gamma_5\partial_\mu\boldsymbol{\phi}\cdot\boldsymbol{\tau}\psi(\mathbf{p}) \qquad (3.54)
\end{aligned}
$$

here $F_2(k^2)=F_{\Lambda\Lambda\gamma}$,form factor at gamma-lambda-lambda vertex.
Converting above Eq.(3.54) into CGLN form we obtain

$$F_1(b) \ =$$

$$\frac{F_{\Lambda\Lambda\gamma}}{f}F_{pK^+\Lambda}\frac{\chi_L}{2m_\Lambda}\frac{1}{p'^2-m_\Lambda^2}\sqrt{\frac{(E''+m_\Lambda)}{2m_\Lambda}\frac{(E+m_p)}{2m_p}}C^{\tau_\Lambda,\tau_K,\tau_p}_{m_{\tau_\Lambda},m_{\tau_K},m_{\tau_\Lambda}+m_{\tau_K}}$$
$$\left\{k\left[-q^2-q_0\left(\frac{k^2+\boldsymbol{q}\cdot\boldsymbol{k}}{E+m_p}\right)-(p'_0-m_\Lambda)\left(q_0+\frac{\boldsymbol{q}\cdot\boldsymbol{k}}{E+m_p}\right)\right]\right.$$
$$+k\frac{q^2}{E''+m_p}\left[(p'_0+m_\Lambda)-q_0+\frac{k^2}{E+m_p}\right]$$
$$+\ k^2\left[\left(-q_0-\frac{q^2}{E''+m_\Lambda}-\frac{q^2}{E+m_p}\right)-(p'_0+m_\Lambda)\frac{q_0}{E+m_p}\right]$$
$$\left.-\ k^2\frac{\boldsymbol{q}\cdot\boldsymbol{k}}{E+m_p}\right\} \tag{3.55}$$

$$F_2(b) \ =$$
$$qk\frac{F_{\Lambda\Lambda\gamma}}{f}F_{pK^+\Lambda}\frac{\chi_L}{2m_\Lambda}\frac{1}{p'^2-m_\Lambda^2}\sqrt{\frac{(E''+m_\Lambda)}{2m_\Lambda}\frac{(E+m_p)}{2m_p}}$$
$$C^{\tau_\Lambda,\tau_K,\tau_p}_{m_{\tau_\Lambda},m_{\tau_K},m_{\tau_\Lambda}+m_{\tau_K}}\left\{k\left[\frac{q^2+2\boldsymbol{q}\cdot\boldsymbol{k}}{(E''+m_\Lambda)(E+m_p)}+\frac{q_0}{E''+m_\Lambda}-1\right.\right.$$
$$\left.+\frac{q_0(p'_0+m_\Lambda)}{(E''+m_\Lambda)(E+m_p)}\right]\left[-(p'_0+m_\Lambda)+\frac{(p'_0-m_\Lambda)}{E''+m_\Lambda}(q_0+\right.$$
$$\left.\left.\frac{\boldsymbol{q}\cdot\boldsymbol{k}}{E+m_p}\right)+\frac{q^2}{E''+m_\Lambda}-q_0+q_0\frac{(k^2+\boldsymbol{q}\cdot\boldsymbol{k})}{(E''+m_\Lambda)(E+m_p)}\right]\right\} \tag{3.56}$$

$$F_3(b) \ =$$
$$qk\frac{F_{\Lambda\Lambda\gamma}}{f}F_{pK^+\Lambda}\frac{\chi_L}{2m_\Lambda}\frac{1}{p'^2-m_\Lambda^2}\sqrt{\frac{(E''+m_\Lambda)}{2m_\Lambda}\frac{(E+m_p)}{2m_p}}$$
$$C^{\tau_\Lambda,\tau_K,\tau_p}_{m_{\tau_\Lambda},m_{\tau_K},m_{\tau_\Lambda}+m_{\tau_K}}\left[\frac{-k}{E+m_p}(q_0+(p'_0-m_\Lambda)+k)\right] \tag{3.57}$$

$$F_4(b) \ =$$
$$q^2\frac{F_{\Lambda\Lambda\gamma}}{f}F_{pK^+\Lambda}\frac{\chi_L}{2m_\Lambda}\frac{1}{p'^2-m_\Lambda^2}\sqrt{\frac{(E''+m_\Lambda)}{2m_\Lambda}\frac{(E+m_p)}{2m_p}}$$
$$C^{\tau_\Lambda,\tau_K,\tau_p}_{m_{\tau_\Lambda},m_{\tau_K},m_{\tau_\Lambda}+m_{\tau_K}}\left\{\frac{-2k}{E''+m_p}\left[-q_0+(p'_0+m_\Lambda)+\frac{k^2}{E+m_p}\right]\right.$$
$$+\ \left.\frac{k^2}{E''+m_\Lambda}\left[2-\frac{q_0}{E+m_p}-\frac{(p'_0-m_\Lambda)}{E+m_p}\right]\right\}. \tag{3.58}$$

In a similar way, the amplitude for the seagull diagram (Fig.3.1c) may be written as

$$\mathcal{M}_1(c) = ie\frac{F_{p\Lambda K^+\gamma}}{f}\bar{\psi}_\Lambda(\mathbf{p}'')\gamma^\mu\gamma_5\mathbf{A}_\mu\boldsymbol{\phi}\cdot\boldsymbol{\tau}\psi_\mathbf{N}(\mathbf{p}) \tag{3.59}$$

which in CGLN form, reads as :

$$F_1(c) = -e\frac{F_{p\Lambda K^+\gamma}}{f}\sqrt{\frac{(E''+m_\Lambda)}{2m_\Lambda}\frac{(E+m_p)}{2m_p}}C^{\tau_\Lambda,\tau_K,\tau_p}_{m_{\tau_\Lambda},m_{\tau_K},m_{\tau_\Lambda}+m_{\tau_K}} \tag{3.60}$$

$$F_2(c) = -e\frac{F_{p\Lambda K^+\gamma}}{f}\sqrt{\frac{(E''+m_\Lambda)}{2m_\Lambda}\frac{(E+m_p)}{2m_p}}C^{\tau_\Lambda,\tau_K,\tau_p}_{m_{\tau_\Lambda},m_{\tau_K},m_{\tau_\Lambda}+m_{\tau_K}} \left[\frac{qk}{(E+m_p)(E''+m_\Lambda)}\right] \tag{3.61}$$

$$F_3(c) = 0, \qquad F_4(c) = 0. \tag{3.62}$$

Where, quark model form factor $F_{p\Lambda K^+\gamma}$ is used for $p\Lambda K^+$ $\gamma$ vertex at the difference of absolute values of photon and kaon momenta.

The diagram (3.1d) represents the interaction when $K^+$ is emitted first which subsequently on interacting with the incoming photon creates a final kaon. The momentum of intermediate $K^+$ is $\boldsymbol{q} = -\boldsymbol{k} + \boldsymbol{q}$

The amplitude may be written as:

$$\mathcal{M}_{K^+}(d) = ie\frac{f_{p\Lambda K^+}}{f}f_{\gamma K^+K^+}A^\nu\boldsymbol{\phi}\partial_\nu\boldsymbol{\phi}\bar{\psi}_\Lambda(\mathbf{p}'')\gamma^\mu\gamma_5\partial_\mu\boldsymbol{\phi}\psi_\mathbf{p}(\mathbf{p}), \tag{3.63}$$

which on solving wears the following CGLN form

$$F_3(d) = -2e\frac{F_{p\Lambda K^+}}{f}F_{\gamma K^+K^+}\sqrt{\frac{(E''+m_\Lambda)}{2m_\Lambda}\frac{(E+m_p)}{2m_p}}C^{\tau_\Lambda,\tau_K,\tau_p}_{m_{\tau_\Lambda},m_{\tau_K},m_{\tau_\Lambda}+m_{\tau_K}} \left(\frac{qk}{q'^2-m^2_{K^+}}\right)\left[\frac{(q_0-k_0)}{E+m_p}-1+\frac{q^2}{(E''+m_\Lambda)(E+m_p)}\right] \tag{3.64}$$

$$F_4(d) =$$

$$-2e\frac{F_{p\Lambda K^+}}{f}F_{\gamma K^+K^+}\sqrt{\frac{(E''+m_\Lambda)}{2m_\Lambda}\frac{(E+m_p)}{2m_p}}C^{\tau_\Lambda,\tau_K,\tau_p}_{m_{\tau_\Lambda},m_{\tau_K},m_{\tau_\Lambda}+m_{\tau_K}}$$

$$\left(\frac{q^2}{q'^2-m^2_{K^+}}\right)\left[\frac{(q_0-k_0)}{E+m_p}+1-\frac{k^2}{(E''+m_\Lambda)(E+m_p)}\right] \qquad (3.65)$$

$$F_1(d)=0, \qquad F_2(d)=0. \qquad (3.66)$$

In the above expressions,the coupling constant is absorbed in the form factor at proton-kaon-lambda vertex, so that if momentum transfer is zero,the form factor is equal to coupling constant at the particular vertex.

## 3.4 Cross Section

To obtain the cross section, amplitude of all the five diagrams must be added and then squared, to get the the transition matrix $\mathcal{M}_{fi}$, that is,

$$\begin{aligned}|\mathcal{M}_{fi}|^2 &= |\mathcal{M}(a)+\mathcal{M}(b)+\mathcal{M}(c)+\mathcal{M}(d)|^2 \\ &= 2\left[(F_1^2+F_2^2)|\epsilon|^2+(F_3^2+F_4^2)(\hat{\mathbf{q}}\cdot\epsilon)^2+2F_1F_2\,(\hat{\mathbf{k}}\cdot\hat{\mathbf{q}})|\epsilon|^2+\right. \\ &\quad \left. 2F_1F_4(\hat{\mathbf{q}}\cdot\epsilon)^2+2F_2F_3\,(\hat{\mathbf{q}}\cdot\epsilon)^2+2F_3F_4(\hat{\mathbf{q}}\cdot\epsilon)^2(\hat{\mathbf{k}}\cdot\hat{\mathbf{q}})\right], \qquad (3.67)\end{aligned}$$

which after summing over initial and averaging over final-channel is used to write the scattering cross-section for $\gamma$ p $\rightarrow$K$^+$ $\Lambda$ as:

$$\frac{d\sigma}{d\Omega}|_{CM}=\frac{1}{64\pi^2}\frac{q}{k}\frac{m_p}{\sqrt{s}E''}\,|\mathcal{M}|^2_{fi}\,. \qquad (3.68)$$

Where $\sqrt{s}$ is the total energy of the $\gamma$-p in the initial and of K$^+$-$\Lambda$ system in the final channel, defined as:

$$\sqrt{s}=\sqrt{m_p^2+k^2}+k=\sqrt{m_\Lambda^2+q^2}+\sqrt{m_{K^+}^2+q^2}. \qquad (3.69)$$

Where $m_p$, $m_\Lambda$ and $m_{K^+}$ indicates the mass of proton, lambda and kaon respectively. Comparing s in, both CM and lab. frame the CM momentum k is given as:

$$\mathbf{k}=\mathbf{k}_{lab}\sqrt{\frac{m_p}{m_p+2\mathbf{k}_{lab}}}, \qquad (3.70)$$

using conservation of energy, we may obtain the CM momentum of the outgoing kaon as

$$|\mathbf{q}| \approx \frac{\sqrt{(s - m_\Lambda^2 - m_{K^+}^2) - 4m_\Lambda^2 m_{K^+}^2}}{2\sqrt{s}} \tag{3.71}$$

# Chapter 4

# Results and Discussion

In this chapter we represent our result for $\gamma$+p$\rightarrow$K$^+$ $\Lambda$ process. We caculate the form factors at different vertices ($\gamma$pp, $\gamma\Lambda\Lambda$ and pK$^+$ $\Lambda$) within the quark model framework, as mentioned in the last chapter (See Eqs. 3.35, 3.37 and 3.39). These form factors are plotted in Fig.3.5 as a function of momentum transfer which account for the composite nature of the baryons.

We use these form factors as a basic ingradient to calculate CGLN amplitudes, for various diagrams contributing to $\gamma$+p$\rightarrow$K$^+\Lambda$ process (Fig.3.1). The CGLN amplitude for each diagram in Fig.3.1 was calculated using CM frame of reference.

We present our calculation of the differential cross sections for $\gamma$+p$\rightarrow$K$^+\Lambda$ reaction at $E_{\gamma lab}$=1.2 GeV and at $E_{\gamma lab}$=1.4 GeV as a function of K$^+$ scattering angle ($\cos\theta_{CM}$)in Fig.4.1, where the data come from ref. [5]. In Fig.4.2, we show the differential cross section as a function of energy at $\theta_{CM}$=90° and $\theta_{CM}$=120°. The data here also come from ref. [5]. The thick solid line takes into account all the four diagrams contributing to $\gamma$+p$\rightarrow$K$^+\Lambda$ and the thin solid line is without the contribution from seagull diagram. The thin dotted line represents the contribution without the diagram 4 in Fig.3.1 and the lower thick dotted line is without the contribution from seagull diagram and diagram 4 in Fig.3.1. Similar is the presentation in Fig.4.2.

The differential cross section shows a forward peaking at both $E_{\gamma lab}$=1.2 GeV and $E_{\gamma lab}$=1.4 GeV, as shown Fig.4.1 this comes from the dominance of the seagull term. It is clear that the seagull term dominates and that without it, results are closer to the experimental data. The form factor used for the seagull diagram at $\gamma$K$^+\Lambda$ vertex is written as a function of momentum transfer (k $-$ q) i.e. F((k $-$ q)). The magnitute of (k $-$ q)=$\sqrt{k^2 + q^2 - 2kqcos\theta}$ in the forward scattering region is close to k-q at small

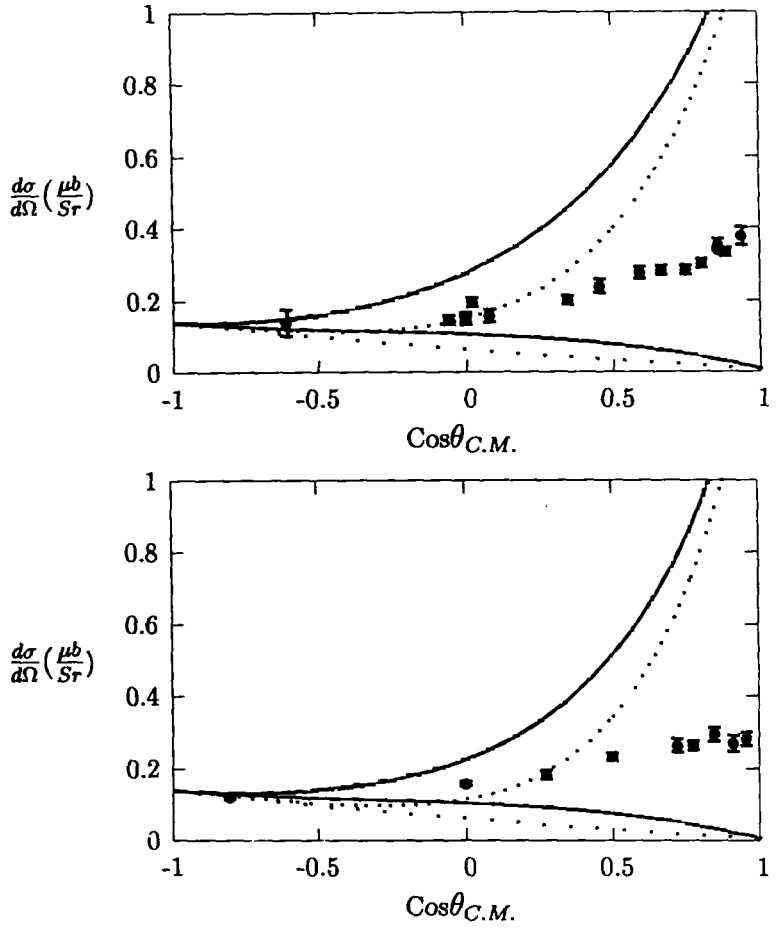


Figure 4.1: The $\gamma p \rightarrow K^+\Lambda$ differential cross section as a function of $K^+$ scattering angle. The upper pannel is at $E_\gamma$=1.2 GeV and the lower pannel is at $E_\gamma$=1.4 GeV . The data is from Ref. [5].

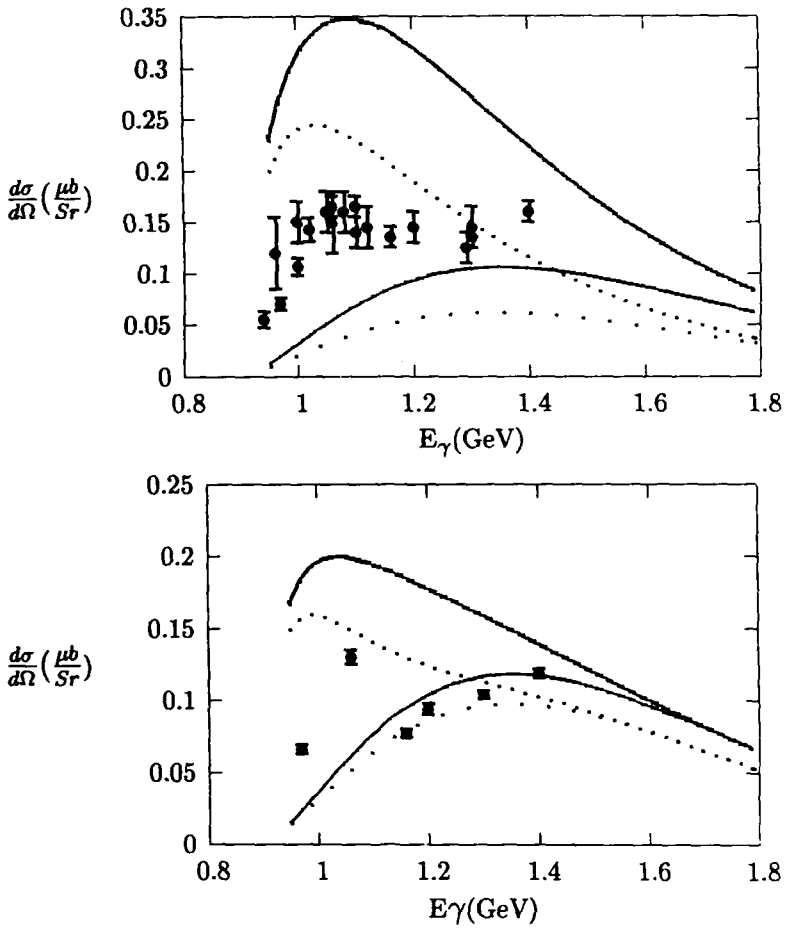


Figure 4.2: The $\gamma p \rightarrow K^+\Lambda$ differential cross section as a function of photon energy. The upper pannel is at $\theta_{C.M.} = 90°$ and the lower pannel is at $\theta_{C.M.} = 120°$. The data is from Ref. [5].

angles where $F((\mathbf{k}-\mathbf{q}))$ is having larger values which is responsible for overshooting of differential cross-section at small angles.

Moreover it can be shown that in ithe chiral quark model [63] the forward peaking behaviour is quite general in the low-energy region for charged meson production because of the dominance of the seagull term, while the seagull term for neutral meson production is zero so that one does not see a strong forward peaking phenomena. This is consistent with the differential cross section data [65] in $\eta$ meson production, which show a little backward peaking above threshold.

The predicted excitation functions shown in Fig.4.2 follow the trend of the data but in magnitude it is above the data and falling off gradually beyond $E_{\gamma lab}$=1.3 GeV. The reason may be that we did not include any resonance. So in this regard phenomenological calculations require the additionof a good number of resoances at different energies to obtain an excitation function which does not fall off rapidly as a function of energy, while our calculation does not exhibit a rapid falloff with energy. The difference may be arising due to use of form factors derived from quark wave functions.

# Bibliography


[1] P. Stassart and F. Stancu, Phys. Rev. **D42**, 1521 (1990).

[2] L. Glosman and D. Riska, Phys. Rep. **268**, 264 (1996).

[3] S. Capstick and W. Roberts, Phys. Rev. **D58**, 074011 (1998).

[4] U. Löring, B. Metsch and H. Petry, Eur. Phys. J. **A10**, 395 (2001).

[5] R. A. Adelseck and B. Saghai, Phys. Rev. **C42**, 108 (1990).

[6] R. A. Williams, C. R. Ji and S. R. Cotanch, Phys. Rev. **C46**, 1617 (1992).

[7] J. Cohen, Int. J. Mod. Phys. **A4**, 1 (1989).

[8] T. Kuo, Phys. Rev. **130**, 1537 (1963).

[9] H. Thom, Phys. Rev. **151**, 1322 (1966).

[10] R. Adelseck and B. Saghai, Phys. Rev. **C45**, 2030 (1992).

[11] R. Adelseck, C. Bennhold and L. Wright, Phys. Rev. **C32**, 1681 (1985).

[12] F. Renard and Y. Renard, Nucl. Phys. **B25**, 490 (1970); Y. Renard ibid **40**, 499 (1972).

[13] R. A. Williams, C. R. Ji and S. R. Cotanch, Phys. Scripta**48**, 217 (1993).

[14] T. Mart, C.Bennhold and C. Hyde-Wright, Phys. Rev. **C51**, 1074(R) (1995).

[15] J. David, C. Fayard, G. Lamot and B. Saghai, Phys. Rev. **C53**, 2613 (1996).

[16] M. Cheoun, B. Han, B.Yu and I.T. Cheon Phys. Rev. **C54**, 1811 (1996).

[17] T. Mizutani, C. Fayard, G. Lamot and B. Saghai, Phys. Rev. **C58**, 75 (1998).

[18] M. Guidal, J.M. Laget and M. Vanderhaeghen, Nucl.Phys. **A627**, 645 (1997).

[19] P. Donoho and R. Walker, Phys. Rev. **112**, 981 (1958).

[20] T. Fuji etal., Phys. Rev. **D2**, 439 (1970).

[21] R. L. Anderson etal., Phys. Rev. Lett.**9**, 131 (1962).

[22] K. H. Althoff etal., Nucl. Phys. **B137**, 269 (1978).

[23] A. Bleckmann etal., Z. Phys. **239**, 1 (1970).

[24] M. Bockhorst etal., Z. Phys. **C63**, 37 (1994).

[25] M. Q. Tran et al., Phys. Lett. **B445**, 20 (1998), http://lisa12.physik.uni-bonn.de/saphir/klks.txt.

[26] S. Goers etal., Phys. Lett. **B464**, 331 (1999), http://lisa12.physik.uni-bonn.de/saphir/web-values-k0si.txt.

[27] B. Borgia etal., Nuovo Cimento **32**, 218 (1964); M. Grilli etal., ibid **38**, 1467, (1965); D. E. Groom and J. H. Marshall, Phys. Rev. **159**, 1213 (1967); R. Hass etal., Nucl. Phys . **B137**, 261 (1978).

[28] J. Ramon, N. Kaiser, S. Wetzel and W. Weise, Nucl. Phys. **A672**, 249 (2000).

[29] E. Oset, J. Nacher, E. Marco, J. Oller, J. Pelaez, A. Ramos and H. Toki, Prog. part. Nucl. Phys.**44**, 243 (2000).

[30] T. Mart and C.Bennhold, Phys. Rev. **C61**, (R)012201 (2000).

[31] S. S. Hsiao and S. R. Cotanch, Phys. Rev. **C28**, 1668 (1983).

[32] B. Saghai and Z. Li, Eur. Phys. J. **A11**, 217 (2001).

[33] R. Alkofer, S. Ahlig, C. Fischer and M. Oettel, Nucl. Phys.**A680**, 70c (2001).

[34] Q. Zhao, Z. Li and C. Bennhold Phys. Rev. **C58**, 2393 (1998).

[35] M. Benmerrouche, N. C. Mukhopadhyay and J. F. Zhang, Phys. Rev. **D51**, 3237 (1995).

[36] A. Donnachie, "photo- andelectroproduction process", in *High Energy Physics*, Vol.V, E. H. S Burhop, ed., pp. 1-185. Academic, New York, 1972. (QC721 B958h V.5).

[37] G. F. Chew, M. L. Goldberger, F. E. Low and Y. Nambu, Phys. Rev. **106**, 1345 (1957).

[38] F. A. Berends, A. Donnachie and D. L. Weaver, Nucl. Phys. **B4**, 103 (1967).

[39] C. Bennhold and L. E. Wright, Phys. Rev. **C36**, 438 (1987).

[40] C. Bennhold, Phys. Rev. **C39**, 1994 (1989).

[41] R. A. Adelseck and L. E. Wright, Phys. Rev. **C38**, 1965 (1988).

[42] B. Saghai and F. Tabakin, Phys. Rev. **C53**, 66 (1996).

[43] M. Gourdin and J. Dufour, Nuovo Cimento **26**, 1410 (1963).

[44] B. Saghai and F. Tabakin, Phys. Rev. **C55**, 917 (1997).

[45] S. Hatsukade and H. J. Schnitzer, Phys. Rev. **128**, 468 (1962); S. Hatsukade and H. J. Schnitzer, Phys. Rev. **132**, 1301 (1963).

[46] N. F. Nelipa and V. A. Tsarev, Nucl. Phys. **45**, 665 (1963); N. F. Nelipa and V. A. Tsarev, Nucl. Phys. **55**, 155 (1964); N. F. Nelipa, Nucl. Phys. **82**, 680 (1966).

[47] W. Schorsch, J. Tietge and W. Weilnbock, Nucl. Phys. **B25**, 179 (1970).

[48] A. Kumar, Ph.D Thesis, Ohio University (1994).

[49] J. F. Zhang, N. C. Mukhopadhyay and M. Benmerrouche Phys. Rev. **C52**, 1134 (1995).

[50] D. Lu, R. Landau and S. C. Phatak, Phys. Rev. **C52**, 1662 (1995).

[51] W.T. Chiang, Ph.D Thesis, Pittsburgh University (2000).

[52] W. T. Chiang, F. Tabakin, T. S. Lee and B. Saghai Phys. Lett. **B517**, 101 (2001).

[53] S. Hsiao, D. Lu and S. Yang, Phys. Rev. **C61**, 068201 (2000).

[54] B. Han, M. Cheoun, K. Kim and I. T. Cheon, Nucl. Phys. Rev. **A691**, 713 (2001).

[55] T. Feuster and U. Mosel, Phys. Rev. **C59**, 460 (1999).

[56] M. Gell Mann, M. L. Goldberger and W. Thirring, Phys. Rev. **95** (1955); M. L.Goldberger, Phys. Rev. **99**, 979 (1955).

[57] R. Kronig, J. Op. Soc. Am., **12**, 547 (1926); H. A. Kramers , Artti Congr. Intern. Fisici Como (1927).

[58] A. W. Thomas, W. Weise, The Stucture of the Nucleon, Wiley-VCH (2000).

[59] H. B. Nielson and A. Patkos, Nucl. Phys. **B195**, 137 (1982).

[60] S. Sahu and S. C. Phatak, Mod. Phys. Lett. **A7**, 709 (1992); S. Sahu, Ph.D Thesis, Utkal University Bhubaneshwar (1992).

[61] A. G. Williams and L. R. Dodd, Phys. Rev. **D37**, 1971 (1988).

[62] D. Lu, S. C. Phatak and R. H. Landau, Phys. Rev. **C51**, 2207 (1995).

[63] Z. Li, Phys. Rev. **C52**, 1648 (1995); Z. Li et al., Phys. Rev. **C56**, 1099 (1997).

[64] R. H. Dalitz, Ann. Rev. Nucl. Sci. **13**, 346 (1963).

[65] H. R. Hicks etal., Phys. Rev. **D7**, 2614 (1973).

[66] R. L. Workman Phys. Rev. **C39**, 2456(1989).

[67] A. W. Thomas, Adv. Nucl. Phys.**13**, 1(1984).